This article was downloaded by:
On: *26 January 2011*
Access details: *Access Details: Free Access*
Publisher *Taylor & Francis*
Informa Ltd Registered in England and Wales Registered Number: 1072954 Registered office: Mortimer House, 37-41 Mortimer Street, London W1T 3JH, UK

Liquid Crystals

Publication details, including instructions for authors and subscription information:
http://www.informaworld.com/smpp/title~content=t713926090

Smectogenic dimeric liquid crystals. The preparation and properties of the α,ω-bis(4-*n*-alkylanilinebenzylidine-4'-oxy)alkanes

R. W. Date[ab]; C. T. Imrie[a]; G. R. Luckhurst[a]; J. M. Seddon[ac]
[a] Department of Chemistry, University of Southampton, Southampton, England [b] School of Chemistry, Queen's University Belfast, Belfast, Northern Ireland [c] Department of Chemistry, Imperial College, London, England

To cite this Article Date, R. W. , Imrie, C. T. , Luckhurst, G. R. and Seddon, J. M.(1992) 'Smectogenic dimeric liquid crystals. The preparation and properties of the α,ω-bis(4-*n*-alkylanilinebenzylidine-4'-oxy)alkanes', Liquid Crystals, 12: 2, 203 — 238

To link to this Article: DOI: 10.1080/02678299208030393

URL: http://dx.doi.org/10.1080/02678299208030393

PLEASE SCROLL DOWN FOR ARTICLE

Full terms and conditions of use: http://www.informaworld.com/terms-and-conditions-of-access.pdf

This article may be used for research, teaching and private study purposes. Any substantial or systematic reproduction, re-distribution, re-selling, loan or sub-licensing, systematic supply or distribution in any form to anyone is expressly forbidden.

The publisher does not give any warranty express or implied or make any representation that the contents will be complete or accurate or up to date. The accuracy of any instructions, formulae and drug doses should be independently verified with primary sources. The publisher shall not be liable for any loss, actions, claims, proceedings, demand or costs or damages whatsoever or howsoever caused arising directly or indirectly in connection with or arising out of this material.

LIQUID CRYSTALS, 1992, VOL. 12, NO. 2, 203–238

Smectogenic dimeric liquid crystals

The preparation and properties of the α,ω-bis(4-*n*-alkylanilinebenzylidine-4′-oxy)alkanes

by R. W. DATE†, C. T. IMRIE, G. R. LUCKHURST*
and J. M. SEDDON‡
Department of Chemistry, University of Southampton,
Southampton SO9 5NH, England

(*Received 3 January 1992; accepted 17 March 1992*)

Eleven series of dimeric liquid crystals, namely the α,ω-bis(4-*n*-alkylanilinebenzylidine-4′-oxy)alkanes, have been synthesized and their transitional properties characterized. The number of methylene groups in the flexible core was varied from one to twelve while the length of the terminal alkyl chains was increased from a methyl group to a decyl substituent. The rich smectic polymorphism of this family of compounds was studied using X-ray diffraction and polarizing microscopy; it includes several examples of rare phase transitions, for example, smectic F–smectic A and crystal G–isotropic, as well as novel modulated hexatic phases based on a two dimensional lattice. The transitional properties of a given series, where the length of the terminal chain is held constant while the length and parity of the flexible spacer is varied, exhibit a pronounced alternation. For example, the entropy change at the nematic–isotropic transition exhibits a strong alternation and this has been interpreted in terms of a corresponding alternation in the long range orientational order at the transition. Increasing the spacer length for a given terminal chain promotes nematic behaviour while increasing the terminal chain length for a given spacer promotes smectic behaviour. A simple relationship relating the occurrence of smectic behaviour to the molecular structure is deduced, namely that for smectic properties to be observed the length of the terminal chains must be greater than half the length of the spacer. We discuss this observation in terms of microphase separation into three distinct regions, the aromatic moieties, the terminal chains and the spacers.

1. Introduction

For many years it was considered that low molar mass liquid crystals had to be composed of molecules comprising a single semi-rigid core attached to which were one or two alkyl chains [1]. This is no longer held to be true and there is now a surprising richness of molecular structures known to promote liquid-crystallinity [2]. Of particular interest are dimeric liquid crystals which differ from conventional low molar mass mesogens in that they are composed of molecules consisting of two mesogenic groups joined by a flexible spacer. The interest in this class of mesogen stems not only from their ability to act as model compounds for semi-flexible main chain liquid-crystalline polymers but also from their quite different properties to conventional low molar mass liquid crystals. In consequence a great many series of dimers have been

---

* Author for correspondence.

† Present address: School of Chemistry, Queen's University Belfast, Belfast BT7 1NN, Northern Ireland.

‡ Permanent address: Department of Chemistry, Imperial College, Exhibition Road, London SW7 2AY, England.

reported (see, for example, [3]) and in many cases the smectic tendencies of the monomers are greatly reduced on coupling to form the dimer (see, for example [4]); this observation has been attributed to the increase in the overall molecular flexibility. In fact, at present there are no dimeric compounds that exhibit a rich smectic polymorphism. Our aim, therefore, was to synthesize a series of smectogenic dimers so that we may proceed to investigate the influence of the dimeric structure on smectic phase formation. It is well-known [5] that long terminal alkyl chains promote smectic behaviour, thus we required a dimeric structure in which we could readily vary the lengths of both the spacer and the terminal alkyl chains. These conditions are met by the α,ω-bis(4-*n*-alkylanilinebenzylidine-4′-oxy)alkanes

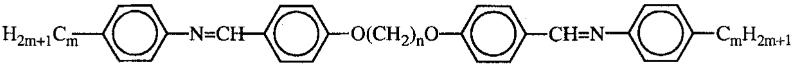

and we consider these compounds to be the dimeric analogues of the extensively studied *N*-(4-*n*-alkyloxybenzylidine)-4′-*n*-alkylanilines

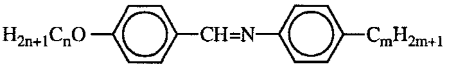

This monomeric series is more commonly referred to as the *n*O.*m*'s where *n* denotes the number of carbon atoms in the alkyloxy chain and *m* that in the alkyl chain. In order to emphasize the monomer-dimer relationship between the α,ω-bis(4-*n*-alkylanilinebenzylidine-4′-oxy)alkanes and the *n*O.*m*'s, the acronym we use to describe the dimers is *m*.O*n*O.*m* where *n* now denotes the number of methylene units in the flexible alkyl spacer and *m* the number of carbon atoms in the terminal alkyl chains. The *m*.O*n*O.*m* family does indeed exhibit a high degree of smectic polymorphism and the smectic phases have been characterized using microscopy and X-ray diffraction. We should note that two members of the *m*.O*n*O.*m* family, 0.O10O.0 and 1.O10O.1 have been reported elsewhere [6].

2. Experimental

The synthetic route for the preparation of the dimers involves two steps; the reaction of 4-hydroxybenzaldehyde with an α,ω-dibromoalkane to produce the α,ω-bis(4-formylphenyl-4′-oxy)alkanes and the subsequent reaction of these with a 4-*n*-alkylaniline to yield the dimers.

2.1. *Synthesis*

2.1.1. *α,ω-Bis(4-formylphenyl-4′-oxy)alkanes*

The members of this series with spacer lengths of 3 up to 10 were prepared using the same method. A mixture of 4-hydroxybenzaldehyde (0·053 mol), an α,ω-dibromoalkane (0·025 mol) and anhydrous potassium carbonate (0·063 mol) in *N*,*N*-dimethylformamide (25 ml) was refluxed with stirring for 3 h. The cooled reaction mixture was then poured into water (300 ml); the resulting precipitate was filtered off and washed thoroughly with water. The crude product was recrystallized twice from ethanol. The eleventh and twelfth homologues were prepared in analogous manner to that described except that ethanol and not DMF was used as the reaction solvent. The methylene homologue was prepared using diiodomethane while the ethylene homologue was prepared by refluxing with sodium in absolute ethanol [7]. The melting points of the aldehydes are in good agreement with the literature values [7].

2.1.2. *4-n-Alkylanilines*

Several of the 4-*n*-alkylanilines used are available commercially and these were redistilled immediately prior to use. The remaining 4-*n*-alkylanilines were prepared using standard procedures described in detail elsewhere [8].

2.1.3. *α,ω-Bis(4-n-alkylanilinebenzylidine-4′-oxy)alkanes*

A 4-*n*-alkylaniline (0·0084 mol) was added to a stirred solution of an α,ω-bis(4-formylphenyl-4′-oxy)alkane (0·004 mol) and a few crystals of *p*-toluene sulphonic acid in hot ethanol; the mixture was allowed to cool to room temperature and stirred for a further 3 h. The resulting precipitate was filtered off, washed thoroughly with cold ethanol and dried. In general, all the *m*.O*n*O.*m* compounds were recrystallized twice from ethyl acetate; the exceptions to this are the even membered materials having terminal chain lengths of 0, 1 and 2 for which toluene was used as the recrystallization solvent. All yields were in excess of 75 per cent and structural characterization of the products was performed using ^{1}H NMR and IR spectroscopy as well as elemental analysis.

2.2. *Thermal characterization*

The thermal behaviour of the *m*.O*n*O.*m*'s was investigated using a Perkin–Elmer DSC-2C differential scanning calorimeter as well as a Nikon polarizing microscope equipped with a Linkam hot stage. This was employed also to study the optical textures of the liquid-crystalline phases. Selected examples of the smectic phases were studied further using X-ray diffraction with a Guinier camera fitted with a bent quartz monochromator (R. Huber, Germany) using CuK$_{\alpha_1}$ radiation ($\lambda = 0{\cdot}15405$ nm). The error in the smectic layer spacings determined from the first order reflection is ±0·3 Å.

3. Results and discussion

The transitional properties of the eleven homologous series of *m*.O*n*O.*m* compounds are given in tables 1 to 11 in the Appendix. Phase identifications were performed using polarizing microscopy and X-ray diffraction. No miscibility experiments have been performed for essentially two reasons; first, X-ray diffraction yields detailed structural information making miscibility studies as a means of phase identification redundant and secondly, the choice of standard materials with which to perform such studies is severely restricted by the high transition temperatures as well as by the novel chemical nature of the *m*.O*n*O.*m* compounds.

3.1. *Phase assignments*

Nematic phases were assigned from their schlieren optical texture which flashed when subjected to mechanical stress, combined with the high mobility of the phase; a typical nematic schlieren texture is shown in plate 1. Smectic A phases have been assigned from optical textures in which regions of focal conic fan and homeotropic textures coexist; an example of this is shown in plate 2. In addition the densitometer scan of the intensity profile of the X-ray diffraction pattern of the smectic A phases shows a first and in some cases a second order Bragg reflection in the low angle region and a diffuse wide angle peak characteristic of a liquid-like arrangement of the molecules within the layers; a typical densitometer scan of an X-ray powder diffraction pattern of a smectic A phase is shown in figure 1.

On cooling the smectic A phase of 4.O4O.4, 5.O4O.5 and 5.O6O.5, the focal conic fans become crossed by bars which were transitory in nature occurring reversibly. The

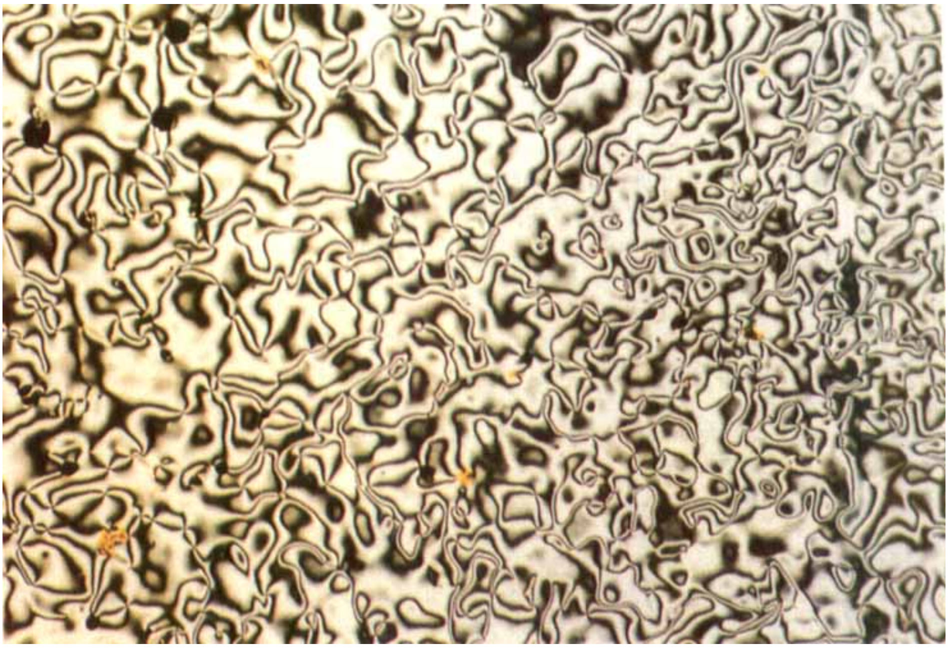

Plate 1. The schlieren texture of the nematic phase exhibited by 7.O10O.7 ($T = 141°C$).

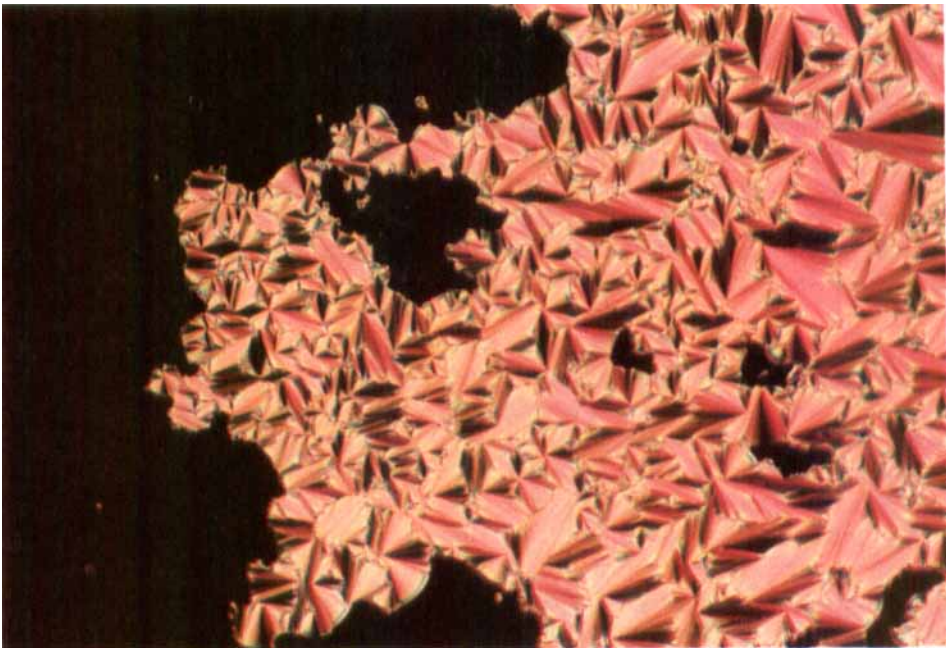

Plate 2. The focal conic fan and homeotropic textures of the smectic A phase exhibited by 5.O4O.5 ($T = 190°C$).

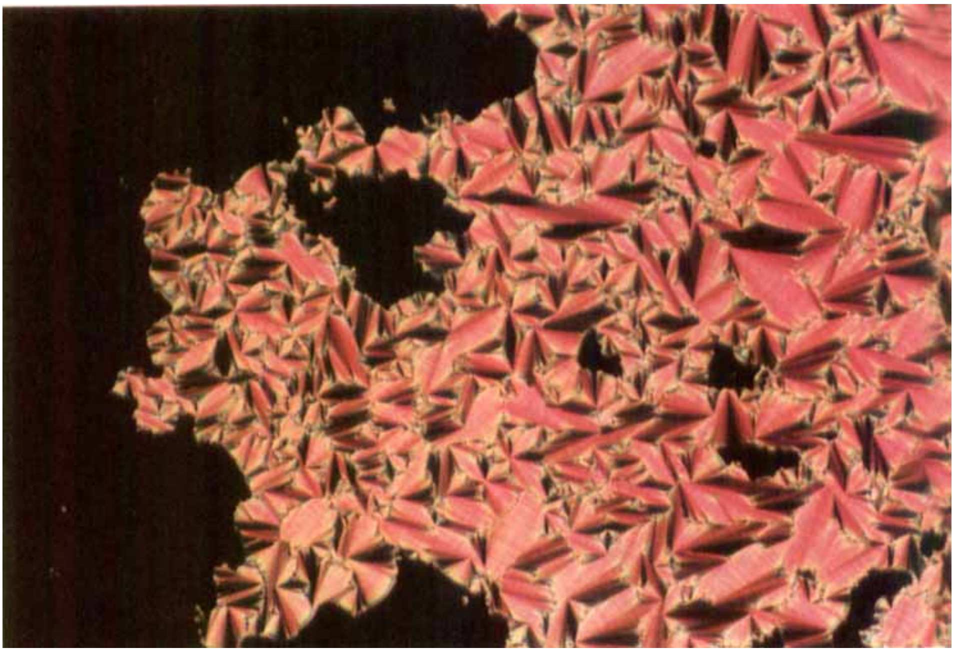

Plate 3. The transition bars observed at the smectic A–smectic B transition of 5.O4O.5 ($T=160°C$).

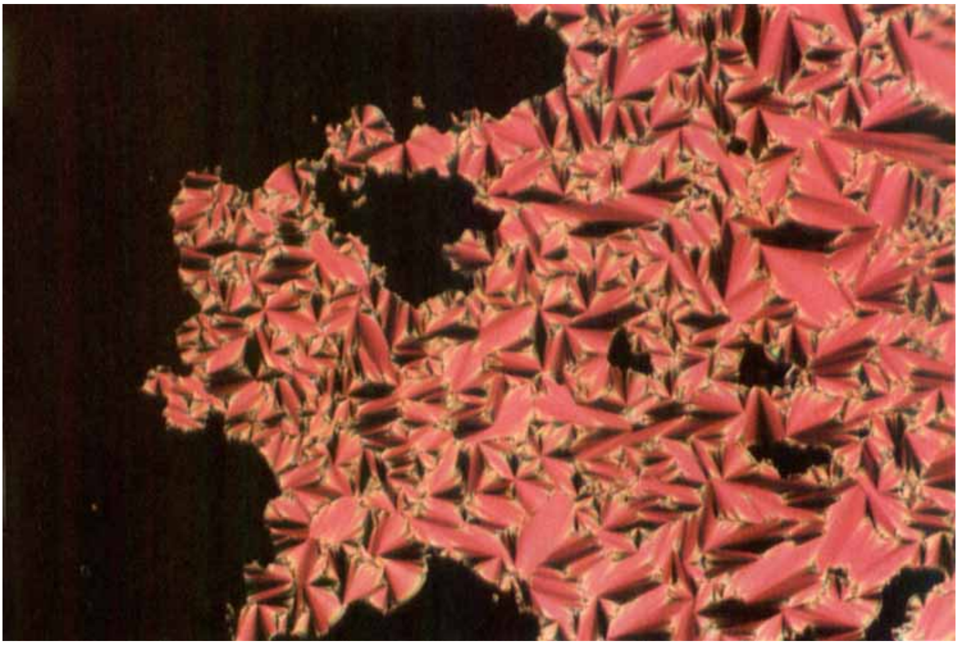

Plate 4. The focal conic fan and homeotropic textures of the smectic B phase exhibited by 5.O4O.5 ($T=155°C$).

Plate 5. The focal conic fan and schlieren optical textures of the smectic C phase exhibited by 10.O6O.10 ($T = 160°C$).

Plate 6. The optical texture of the smectic F phase obtained on cooling the smectic C phase of 10.O6O.10 in plate 5 ($T = 115°C$).

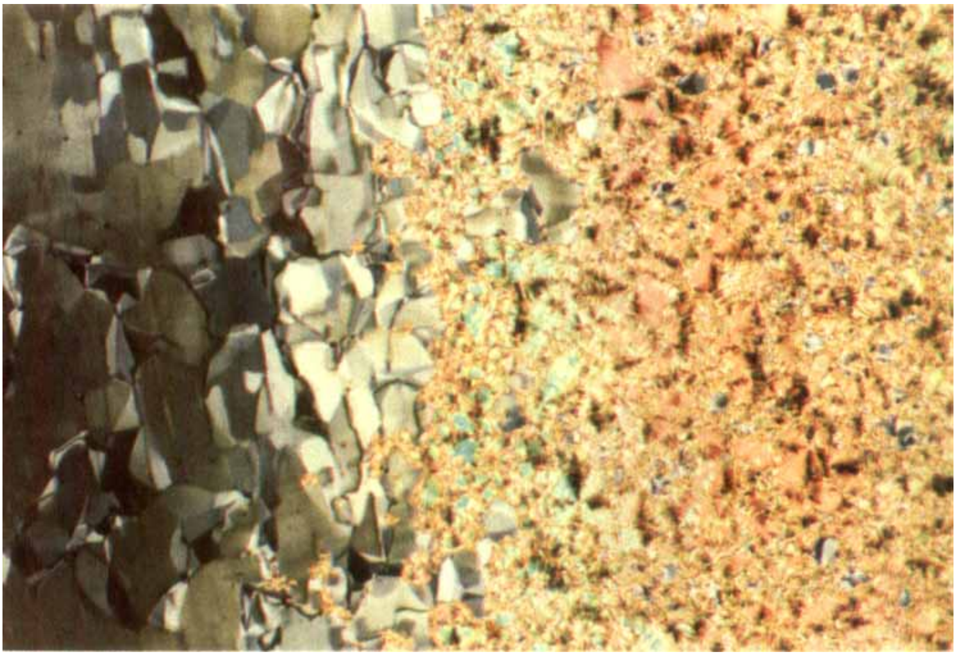

Plate 7. The optical texture of the smectic F phase obtained on cooling the smectic A phase of 7.O4O.7 ($T=115$°C).

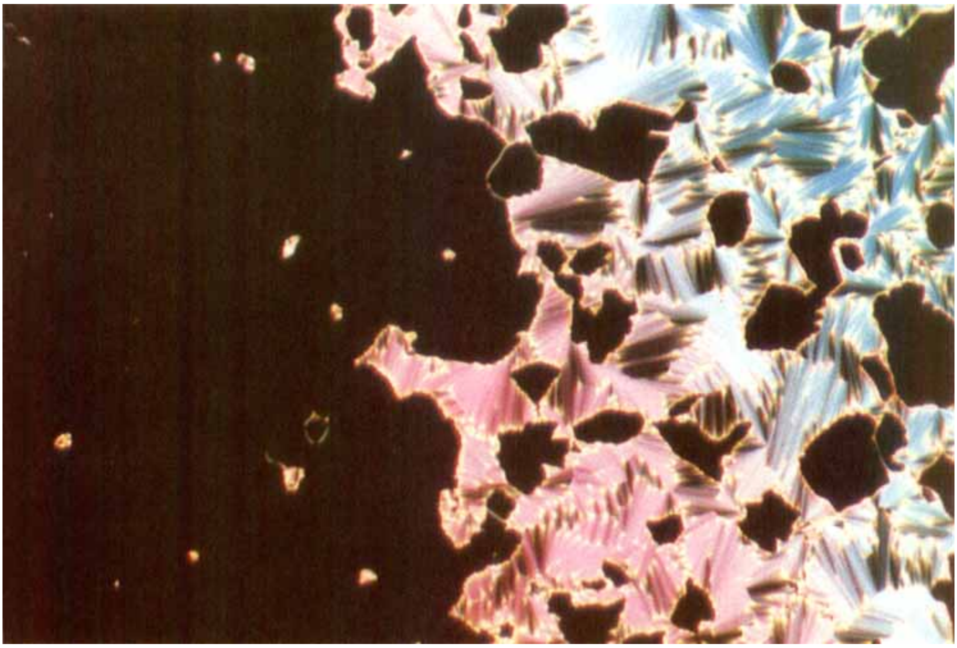

Plate 8. The focal conic fan and homeotropic textures of the smectic A phase exhibited by 7.O10O.7 ($T=133$°C).

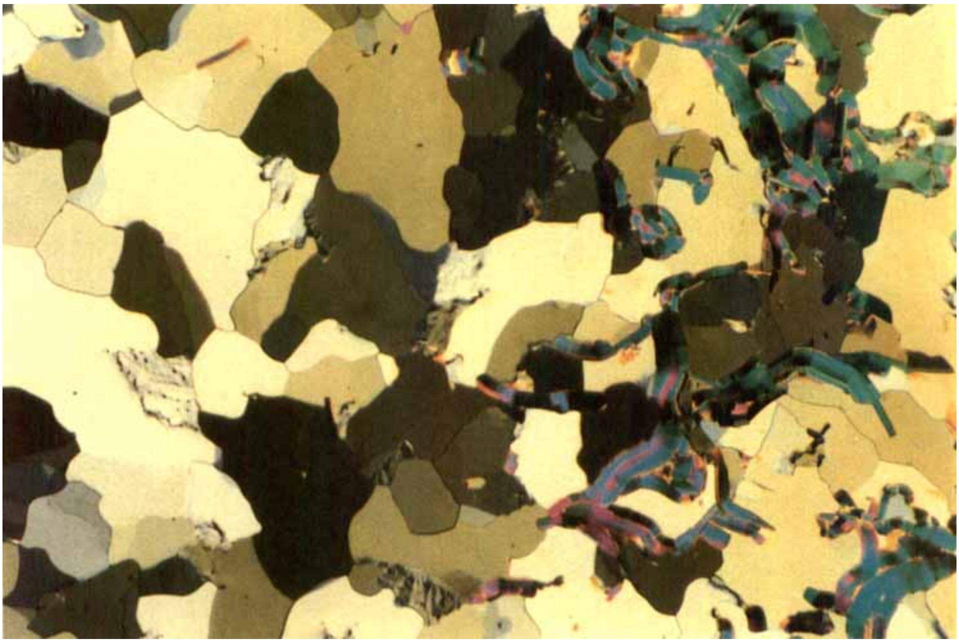

Plate 9. The optical texture of the G/J phase obtained on cooling the smectic A phase of 7.O10O.7 in plate 8 ($T = 126°C$).

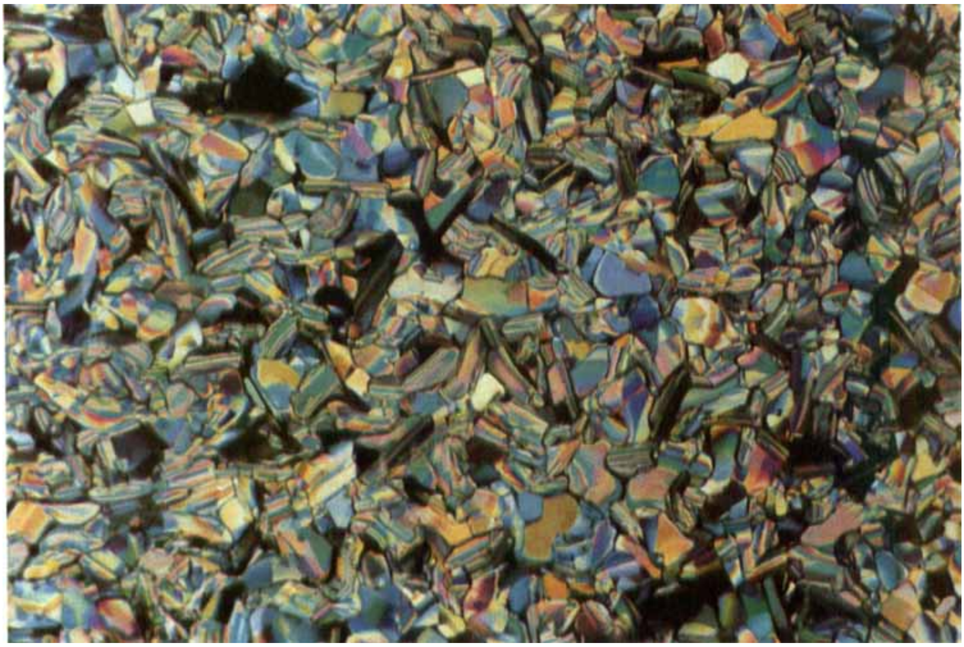

Plate 10. The natural optical texture of the G/J phase of 8.O12O.8 ($T = 125°C$).

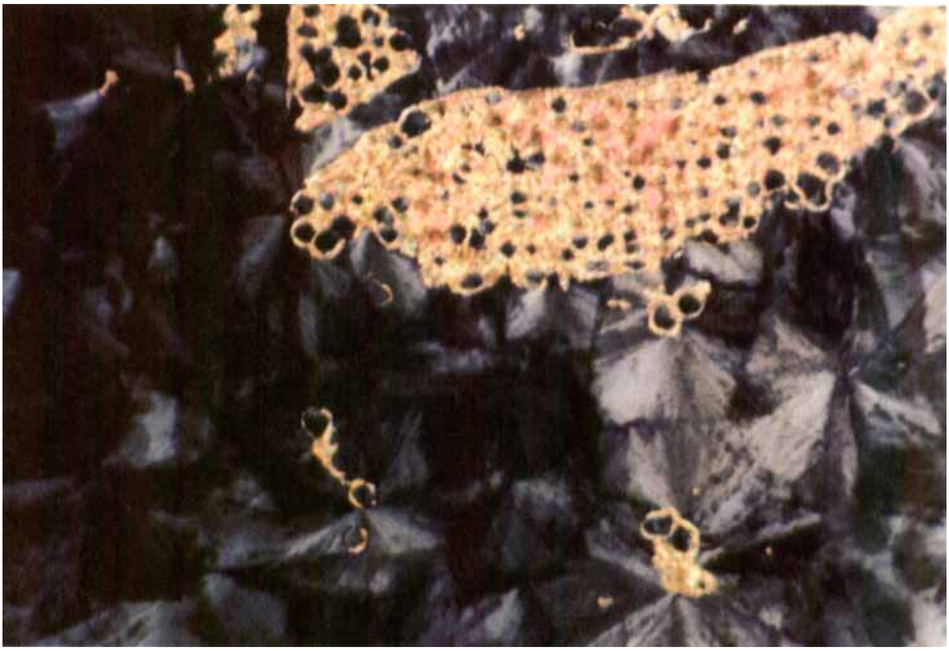

Plate 11. The optical texture of the S_1 phase obtained by cooling the smectic A phase of 10.O9O.10 ($T = 110°C$).

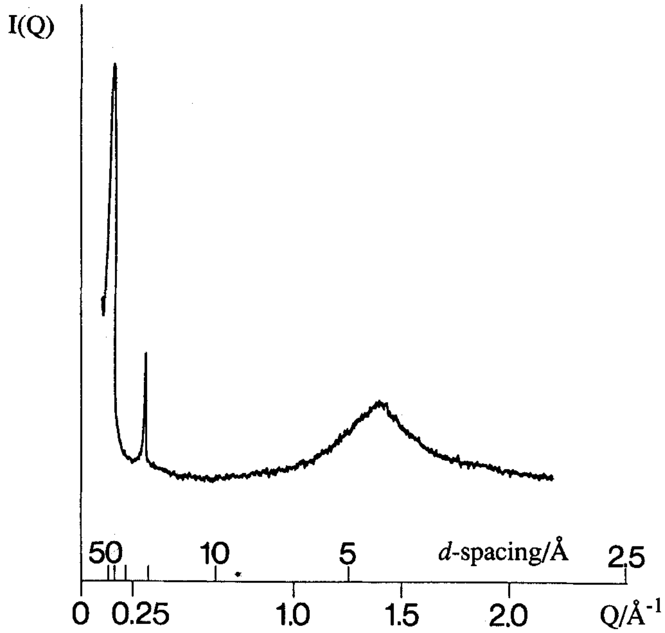

Figure 1. The intensity profile of the X-ray diffraction pattern of the smectic A phase exhibited by 5.O4O.5 ($T = 190°C$).

fans in the lower temperature mesophase are smooth and free of blemishes. This sequence is shown in plates 2, 3 and 4; it is very characteristic of a smectic A to smectic B transition. It should be noted also that the homeotropic regions remained unchanged implying that the orthogonal alignment of the director is maintained. This view is supported by X-ray diffraction. Figure 1 shows the densitometer scan for the smectic A phase of 5.O4O.5; the peak in the wide angle region is clearly very broad and is centred at $Q = 1{\cdot}4\,\text{Å}^{-1}$. The layer spacing or periodicity of the smectic A phase of 5.O4O.5 determined from the first order reflection is 41·4 Å ($T \approx 190°\text{C}$). On cooling the smectic A phase into the lower temperature phase the wide angle diffraction peak narrows considerably (see figure 2) implying the presence of considerably longer range ordering within the layers. The full width at half maximum height of the wide angle peak for the smectic A phase is approximately $0{\cdot}39\,\text{Å}^{-1}$ whereas in the smectic B phase this value is reduced to $0{\cdot}03\,\text{Å}^{-1}$. The layer spacing in the smectic B phase is 42·6 Å which is equal within experimental error to the estimated all *trans* molecular length of 5.O4O.5 of

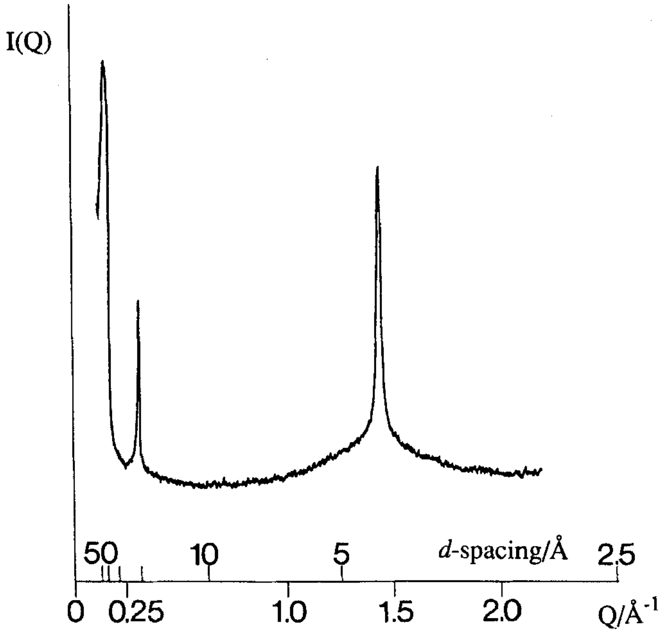

Figure 2. The intensity profile of the X-ray diffraction pattern of the smectic B phase of 5.O4O.5 ($T = 154°\text{C}$).

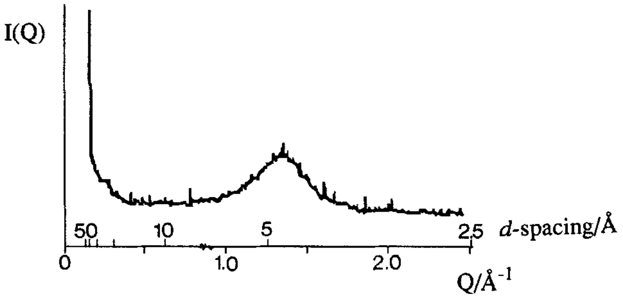

Figure 3. The intensity profile of the X-ray diffraction pattern of the smectic C phase exhibited by 10.O4O.10 ($T = 196°\text{C}$). The first order Bragg peak is over exposed.

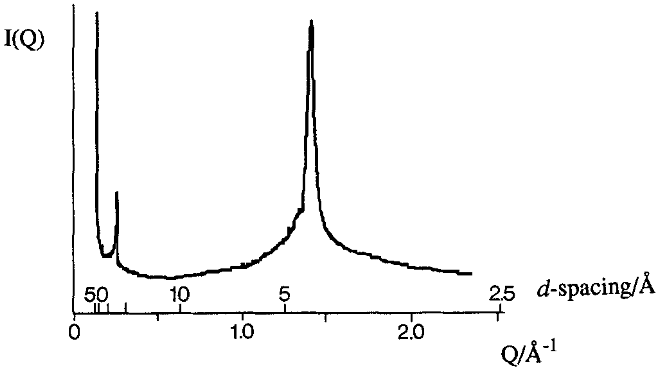

Figure 4. The intensity profile of the X-ray diffraction pattern of the smectic F phase of 10.O4O.10 ($T = 138°C$).

42·0 Å. The hexagonal lattice parameter is 5·25 Å. It is interesting to note that transition bars are not observed for all smectic A–smectic B transitions and it has been suggested that their presence is an indication that the B phase is of the crystal type [9]. However, this is clearly not so for this example because the wide angle band in figure 2 possesses no structure, implying that the phase is a hexatic smectic B.

Smectic C phases were identified by the observation of regions of focal conic fan and schlieren optical textures when viewed through the polarizing microscope. If the smectic C phase was formed on cooling a smectic A phase then the focal conic fans were sanded and broken. However, if the smectic C phase formed directly from the isotropic liquid then the fans appeared clearer. The optical texture of the smectic C phase formed by cooling the smectic A phase of 10.O6O.10 is shown in plate 5. X-ray diffraction supports these assignments; figure 3 shows the densitometer scan of the X-ray

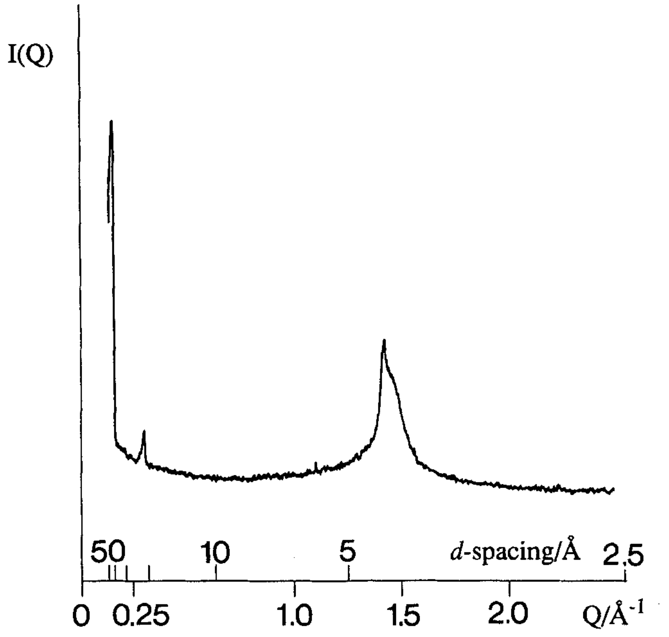

Figure 5. The intensity profile of the X-ray diffraction pattern of the smectic F phase of 7.O5O.7 ($T = 95°C$).

diffraction pattern for the smectic C phase of 10.O4O.10 and a first order diffraction maximum is evident in the low angle region while the wide angle diffraction band is broad. The layer spacing of this phase determined from the first order diffraction maximum is found to be temperature dependent, varying from 47·8 Å at 205°C to 46·1 Å at 171°C. The estimated all *trans* molecular length of 10.O4O.10 is 54 Å.

On cooling the smectic C phase of several *m*.O*n*O.*m* compounds, the breaks in the fans become well-defined changing into black patches while a mosaic schlieren texture develops from the regions of schlieren texture; these textures are shown in plate 6 and were obtained on cooling the sample shown in plate 5. These textural changes are characteristic of a smectic C to a smectic F transition. A densitometer scan of the X-ray diffraction pattern for the lower temperature mesophase of 10.O4O.10, produced by cooling the sample shown in figure 3, is given in figure 4. The scan for the lower temperature phase possesses two orders of diffraction in the low angle region and the wide angle band has been narrowed considerably but does not possess any structure indicating this phase to be a true hexatic smectic. The layer spacing in this lower temperature mesophase is 48 Å ($T \approx 138$°C) and this exhibits a small temperature dependence. The wide angle diffraction band in a smectic F phase is broader than that for a smectic B phase (see figures 2 and 4) and this is a result of the director tilt with respect to the layer normals. We have, therefore, assigned this phase to be a smectic F but stress that X-ray diffraction on powder samples cannot distinguish between the smectic F and I phases and hence this phase could equally be a smectic I. The optical texture for the smectic F phases formed on cooling a smectic A phase consists of finely arced focal conic fans and poorly coloured mosaic platelets with sharply defined boundaries which develop from the homeotropic regions; an example of these textures are shown in plate 7. The X-ray powder diffraction patterns are similar to those described for the smectic F phases produced on cooling a smectic C phase. However, the lower temperature smectic phase exhibited by 7.O4O.7 has been studied by X-ray diffraction using aligned samples and this revealed the phase to be unambiguously a smectic F phase. Due to the similarity in the optical textures, therefore, we assign all these phases as smectic F phases. A complete description of the X-ray diffraction studies on aligned samples of *m*.O*n*O.*m* compounds will be given elsewhere. An unusual feature in the X-ray diffraction pattern for the smectic F phases exhibited by odd membered compounds is an unresolved shoulder on the peak in the wide angle region; an example of this is shown as figure 5. To our knowledge such a feature has not previously been reported and may arise from a distortion of the hexagonal lattice due to difficulties in packing bent molecules.

On cooling the smectic A phase of, for example, 7.O10O.7 a mosaic texture composed of large poorly coloured areas develops from the homeotropic regions while the focal conic fans become broken giving rise to a patchwork texture; this transition is shown in plates 8 and 9. These textural changes are typical of a smectic A to a crystal G transition. The changes in the X-ray diffraction powder pattern on cooling 7.O10O.7 can be seen in figures 6 and 7; the broad wide angle diffraction band in figure 6 is narrowed considerably on cooling and, in addition, a second order diffraction maximum is present in figure 7 and not in figure 6. It is important to note that the wide angle band in figure 7 possesses structure indicative of a three dimensional arrangement. The layer spacing in the smectic A phase is 50·5 Å ($T \approx 135$°C) and in the lower temperature mesophase is 40·8 Å ($T \approx 125$°C); the estimated all *trans* molecular length of 7.O10O.7 is 53·0 Å. Therefore, we assign this lower temperature phase as a crystal G with the reservation that it may be a crystal J; we hope to resolve this ambiguity using

X-ray diffraction of aligned samples. The crystal G phase formed directly from the isotropic liquid has similar X-ray powder diffraction patterns but exhibits an optical texture consisting of elongated platelets which separate from the isotropic phase as splinters, see plate 10.

The compounds 10.O9O.10 and 10.O11O.10 have been found to exhibit novel types of smectic phases. Both compounds form an enantiotropic phase denoted S_1 below the S_A phase, whilst 10.O9O.10 has a further monotropic phase denoted S_2 below S_1:

$$\begin{tikzcd} \mathrm{C} \arrow[rr, dash, "105^\circ\mathrm{C}"] & & S_1 \arrow[r, dash, "114^\circ\mathrm{C}"] \arrow[dl, "105^\circ\mathrm{C}"] & S_A \arrow[r, dash, "126^\circ\mathrm{C}"] & \mathrm{I}, \\ & S_2 \arrow[ul] & & & \end{tikzcd}$$

10.O9O.10

$$\mathrm{C} \overset{99^\circ\mathrm{C}}{\text{——}} \mathrm{G/J} \overset{104^\circ\mathrm{C}}{\text{——}} S_1 \overset{116^\circ\mathrm{C}}{\text{——}} S_A \overset{118^\circ\mathrm{C}}{\text{——}} \mathrm{I}.$$

10.O11O.10

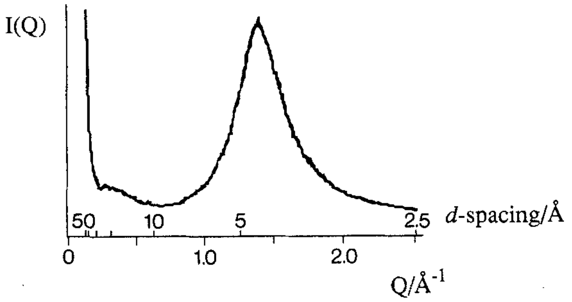

Figure 6. The intensity profile of the X-ray diffraction pattern of the smectic A phase exhibited by 7.O10O.7 ($T = 132$°C). The first order Bragg peak is over exposed.

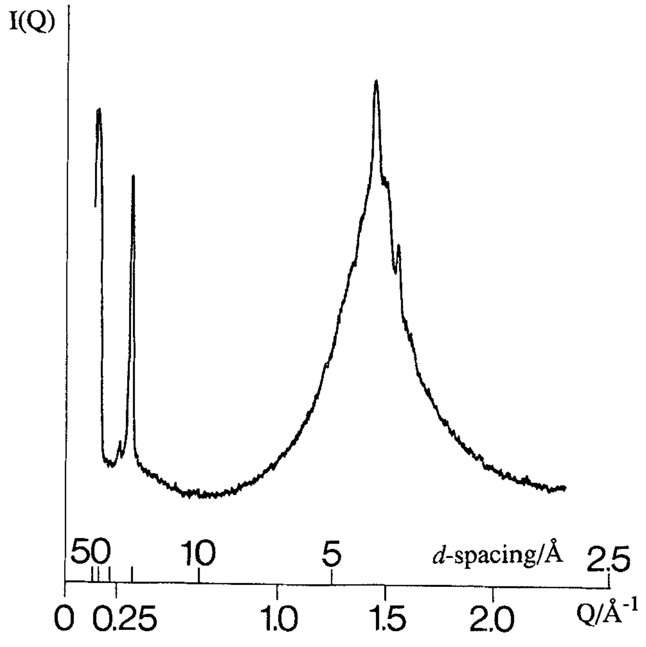

Figure 7. The intensity profile of the X-ray diffraction pattern of the G/J phase exhibited by 7.O10O.7 ($T = 127$°C).

Optical texture studies suggest that they are tilted phases: on cooling from an S_A phase into the S_1 phase, the areas of homeotropic texture transformed into birefringent, poorly defined mosaic regions which formed via dendritic growth, the loss of the homeotropic texture suggesting that the phase is tilted; this texture is shown in plate 11. The optical texture of the S_2 phase is very similar, implying that it too has a tilted structure.

The wide angle powder diffraction patterns are typical of hexatic phases where the molecular packing in a plane normal to the molecular long axis is hexagonal, and the lateral coupling between adjacent layers is weak. For example, the powder pattern of the S_1 phase of 10.O11O.10 at 110°C, shown in figure 8, has a single narrow wide angle peak centred at $Q = 1{\cdot}40\,\text{Å}^{-1}$, with a full width at half maximum height of $\Delta Q = 0{\cdot}11\,\text{Å}^{-1}$. This could be consistent with either an S_B, S_F or S_I phase, although it is slightly broad to be the former. However, the low angle region shows a series of seven sharp Bragg reflections which do not index on a one dimensional lamellar lattice, but rather index on a two dimensional oblique lattice. The observed reflections correspond to $1\bar{1}$, 01, 11, $2\bar{2}$, 02, 12 and 22, respectively. The same modulated S_1 phase is observed for 10.O9O.10, the lattice parameters for the latter compound at 112·5°C are $a = 173{\cdot}3\,\text{Å}$ and $c = 57{\cdot}2\,\text{Å}$, the angle between the lattice vectors being $\beta = 106°$. These parameters are essentially constant over the narrow range of existence of the S_1 phase. Two of the lines appear to be continuous with the first and second order reflections from the S_A phase (see figure 9). The smectic A phase has a layer spacing of 54·6 Å at 114°C (compared to an estimated all *trans* molecular length of 56·0 Å).

The oblique lattice implies that the layers develop a modulated structure, either by breaking up into ribbons, which are then slightly displaced along the *c* direction with

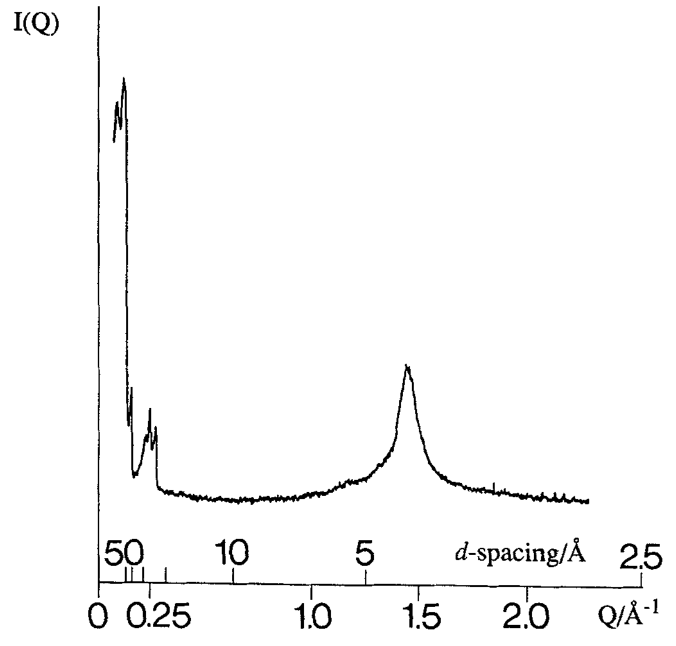

Figure 8. The intensity profile of the X-ray diffraction pattern of the S_1 phase of 10.O11O.10 ($T = 110$°C).

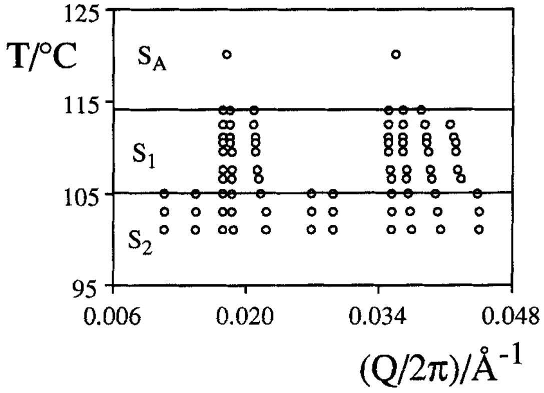

Figure 9. The low angle X-ray reciprocal spacings of 10.O9O.10 as a function of temperature.

respect to the neighbouring ribbons, or by a rippling of the layers, with the ripples having an asymmetric profile. This rippled structure would be essentially the thermotropic analogue of the so-called $P_{\beta'}$ rippled gel phase observed in lyotropic systems such as phospholipids. Modulated smectic structures have been observed in a variety of systems as variants of the S_A and S_C phases. However, there are very few cases where hexatic phases show such behaviour. One example is the compound 4-(4′-cyanobenzyloxy)benzylidene-4″-*n*-nonyloxyaniline, which adopts a modulated S_B structure with a two dimensional oblique lattice [10]. In this case, the ribbons consist of domains in which the asymmetric molecules are aligned either in one direction, or the other.

On cooling the S_1 phase of 10.O9O.10 into the S_2 phase, the wide angle pattern is unchanged, but the low angle pattern changes abruptly, with a total of 11 Bragg reflections being observed. Six of these appear to be continuous in spacing with the reflections observed in the S_1 phase, although this may be accidental; this can be seen in figure 9. The diffraction data for the S_2 phase have not as yet been satisfactorily indexed. It is, however, very likely that the structure is also a modulated hexatic phase based on a two dimensional lattice.

For the compound 10.O11O.10, only the S_1 modulated hexatic phase is observed, with a crystal G or J phase occurring between the S_1 and crystal phases. For this compound, the S_A phase has a layer spacing of 57·1 Å at 118°C, compared to an estimated all *trans* length of 62·0 Å. On cooling into the S_1 phase, a total of 8 low angle Bragg reflections were observed, which index on an oblique lattice of dimensions $a = 147{\cdot}7$ Å, $c = 60{\cdot}6$ Å and $\beta = 115°$ at 116°C. In this case the layer spacing of the S_A phase is not continuous with any of the observed lines of the S_1 phase, suggesting that the apparent continuity for 10.O9O.10 was accidental. The *c* dimension for 10.O11O.10 is some 3 Å larger than that observed for 10.O9O.10, consistent with the additional two methylene groups in the central connecting chain of the former molecule. However, the *a* dimension of the former is actually some 27 Å smaller than the value of 175 Å observed for 10.O9O.10, and the angle β is some 9° larger.

3.2. *The dependence of the transitional properties on the length of the alkyl core*

We turn our attention now to the transitional properties of the *m*.O*n*O.*m* compounds and their relationship to the length of the flexible alkyl core. For the sake of brevity we shall discuss the properties of just three series, one possessing short terminal chains, 2.O*n*O.2, another medium length chains 6.O*n*O.6 and finally long terminal chains 10.O*n*O.10, but we stress that the trends revealed are typical of this whole class of compounds. The behaviour of the 1.O*n*O.1 and 4.O*n*O.4 series have been discussed briefly elsewhere [11, 12].

3.2.1. *2.OnO.2 series*

The dependence of the transition temperatures on the number of methylene units in the flexible core for the 2.O*n*O.2 series is shown in figure 10. All the members of this series exhibit nematic behaviour with the exception of the first member for which no liquid-crystalline behaviour was observed. Both the melting points and the nematic–isotropic transition temperatures show a very large odd–even effect in which the even members have the higher values; in the case of the clearing temperatures this alternation attenuates with increasing core length.

Figure 11 shows the dependence of the entropy change associated with the nematic–isotropic transition on the number of methylene units in the alkyl spacer for the 2.O*n*O.2 series and a dramatic odd–even effect is revealed which does not attenuate on increasing *n*. The entropies of the even members are in most instances several times

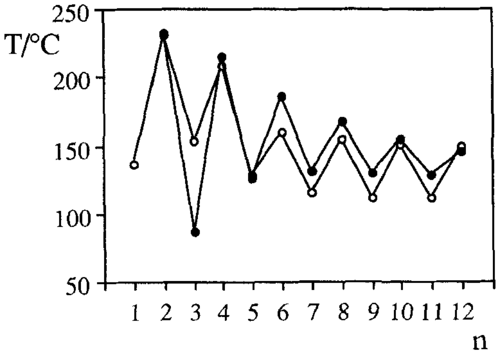

Figure 10. The dependence of the melting points indicated by ○ and the nematic–isotropic transition temperature denoted by ● on the number of methylene groups, *n*, in the flexible alkyl core for the 2.O*n*O.2 series.

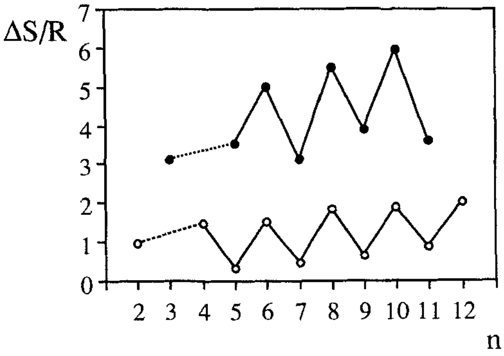

Figure 11. The dependence of the entropy change associated with the nematic–isotropic transition indicated by ○ on the number of methylene groups, *n*, in the flexible alkyl core for the 2.O*n*O.2 series. Also shown are the entropy changes associated with the smectic A–isotropic transition indicated by ● on the number of methylene groups, *n*, in the flexible alkyl core for the 10.O*n*O.10 series.

larger than those of the odd members as well as being considerably greater than those of the monomeric analogues; for example, 2.O12O.2 has a value of $\Delta S_{NI}/R$ of 2·00 whereas the $\Delta S_{NI}/R$ for 6O.2 is just 0·36 [13]. The underlying trend in the entropies for the 2.O*n*O.2 series is an increasing one with increasing *n* and it may be argued that the alternation does attenuate in a relative sense since the values of $\Delta S_{NI}/R$ increase with increasing *n* but the difference in $\Delta S_{NI}/R$ between the *n* and $(n+1)$ homologues appears approximately constant.

The 2.O*n*O.2 series serves as an archetypal example of a homologous series of dimeric liquid crystals; its transitional properties are very typical indeed, namely, the very large alternation in both the nematic–isotropic transition temperatures and entropies on increasing the core length. A somewhat simplistic explanation has been offered by many authors to rationalise these observations (see, for example [6]) which assumes the spacer exists exclusively in an all *trans* conformation in the nematic phase. Thus for even membered spacers the two mesogenic moieties are almost parallel whereas for odd membered spacers they are no longer parallel and instead form an angle of about 108°. It is, however, rather unrealistic to consider only a single conformation of a core repeatedly termed flexible. Indeed if this assumption of a single conformer was correct then the even members of a dimer series would be expected to have an entropy of transition equal to that of a monomer. In contrast the more biaxial, odd members of the dimer series would be expected to have an entropy of transition lower than that of the corresponding monomer [14]. In reality the odd membered dimers have entropies of transition similar to those of the monomers while the even dimers have entropies of transition which are significantly greater. A more tempting plausible explanation rests with the fact that there is a greater number of conformations for the even spacer which preserve the parallelism of the two anisometric units than there is for the odd spacer; this is shown schematically in figure 12. These elongated conformers are more favoured in the nematic environment and hence there should be a greater conformational entropy change for even members than for odd members at the nematic–isotropic transition. It is possible to test this idea at least semi-quantitatively by using the Marcelja–Luckhurst theory of nematics [15] to calculate the conformational and orientational contributions to the entropy change at the nematic–isotropic transition. In this theory the system is treated rather like a multicomponent nematogenic mixture in which the components are the various conformers given by Flory's rotameric state model. The orientational ordering potential for each component is then taken to be analogous to that occurring in the Luckhurst–Zannoni–Nordio–Segre molecular field theory for biaxial particles [14]. The strength of the molecular field experienced by the conformers is related to the geometry of each conformer together with bond or group interaction parameters. For the dimers of interest here these would be, at the simplest level, a single parameter for a Schiff's base mesogenic group and another for the carbon–carbon bonds. That is the flexibility of the terminal alkyl chains would be ignored as would the difference between a carbon–oxygen and a carbon–carbon bond. For the cyanobiphenyl dimers the interaction parameters for the carbon–carbon bond is about 0·2 times that for the mesogenic group. We have used the same ratio in our calculations and have taken the geometry of the chain to be perfectly tetrahedral when calculating how the total interaction tensor for the dimer varies between conformers. The details of such calculations and the basic molecular field theory are given elsewhere; here we are only concerned with the variation of the entropy of transition with the number of methylene groups in the flexible alkyl spacer.

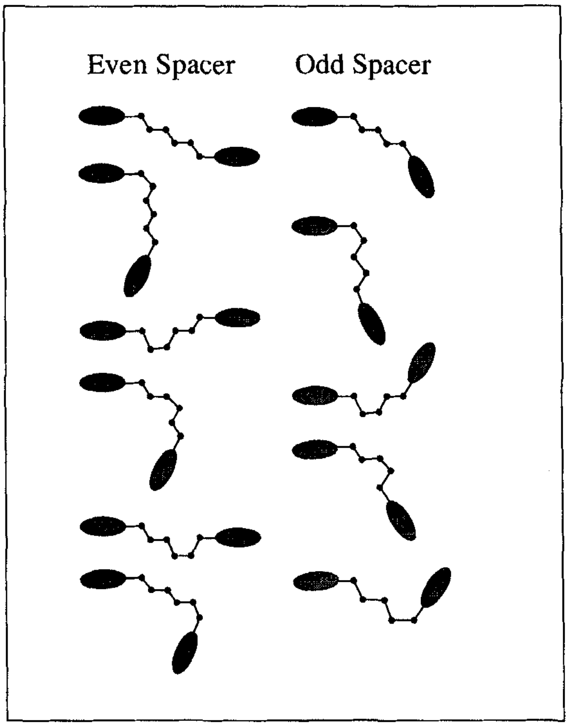

Figure 12. A diagrammatic representation in two dimensions of introducing a single *gauche* defect into the alkyl core of dimeric liquid crystals with even and odd spacers.

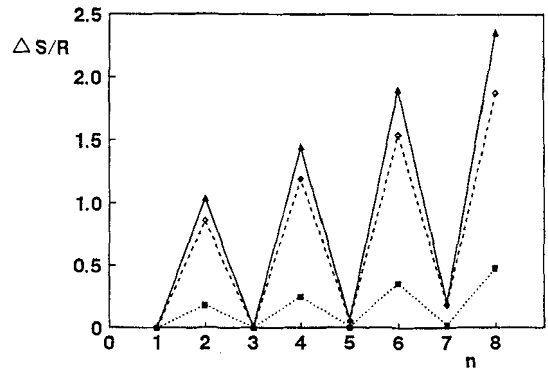

Figure 13. The calculated entropies of transition for the dimers showing the conformational (····), and the orientational (– – –) contributions as well as the total entropy shown (——).

The results of the calculations are shown in figure 13; here we give the total transitional entropy, the contribution resulting from the change in the conformational distribution at the nematic–isotropic transition and that resulting from the disappearance of the long range orientational order at the transition. As we had anticipated the conformational entropy for even members is significantly greater than for odd dimers. In fact the conformational entropy for odd members is vanishingly small. However the conformational contribution for even members is also small amounting to no more than about 20 per cent of the total transitional entropy. The dominant contribution clearly originates from the orientational order and it is this contribution which alternates significantly between odd and even members of the series. The observed alternation of the transitional entropy along a homologous series of dimers should therefore be interpreted essentially in terms of the alternation in the long range orientational order. Indeed such an alternation is found for the second rank order parameter for the long axis of the cyanobiphenyl group of the α,ω-bis(4-cyanobiphenyl-4′-oxy)alkanes [16].

3.2.2. *6.OnO.6 series*

On increasing the terminal chain length to six carbon atoms giving the 6.O*n*O.6 series, smectic phases are observed. In fact, nematic behaviour has been extinguished in the compounds with spacer lengths 2 to 6 and 8. The dependence of the transition temperatures on the length of the core for the 6.O*n*O.6 homologous series is shown in figure 14; again, the clearing temperatures show a marked alternation in which the even members have the higher values and which attenuates with increasing core length. The melting points increase on passing from the first to second member, subsequently decrease to the fifth member and then alternate on increasing the core length. Early members of the 6.O*n*O.6 series exhibit smectic A–isotropic transitions whereas the higher members exhibit purely nematic behaviour; this observation is not in accord with the general result that increasing the length of an alkyl chain promotes smectic behaviour in low molar mass mesogens [5] and that increasing the spacer length in semi-flexible main chain polymers also promotes smectic behaviour [17]; this will be discussed later.

3.2.3. *10.OnO.10 series*

The dependence of the transition temperatures on the length of the flexible core for the 10.O*n*O.10 series is shown in figure 15; all the members of this series are purely smectic with the sole exception of the first member for which no liquid-crystalline behaviour was observed. The clearing points of this series again show a pronounced alternation in which the even members have the higher values and which attenuates on increasing the core length.

Figure 11 shows also the entropy change associated with the smectic A–isotropic transition exhibited by several members of the 10.O*n*O.10 series. The values of $\Delta S_{S_AI}/R$

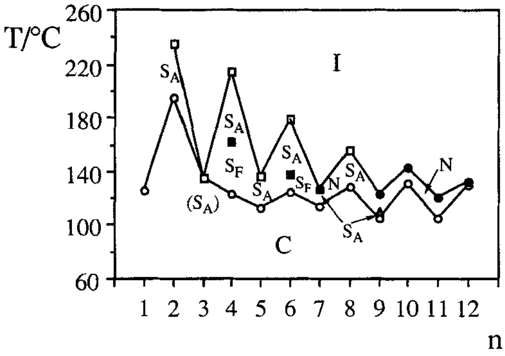

Figure 14. The dependence of the transition temperatures on the length of the flexible alkyl core for the 6.O*n*O.6 series. Melting points are denoted by ○, □ indicate smectic A–isotropic transitions, ● the nematic–isotropic transitions, ■ smectic F–smectic A transitions and △ smectic A–nematic transitions.

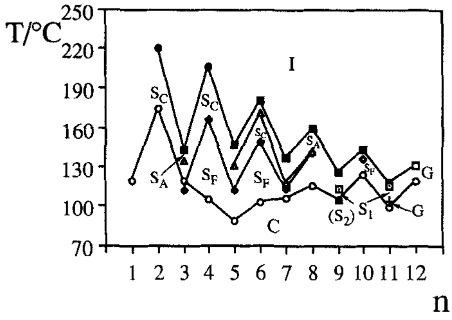

Figure 15. The dependence of the transition temperatures on the length of the flexible alkyl core for the 10.O*n*O.10 series. Melting points are denoted by ○, ● indicate smectic C–isotropic transitions, ■ smectic A–isotropic transitions, □ the crystal G–isotropic transition, △ smectic C–smectic A transitions, ⊡ smectic 1–smectic A transitions, ◆ smectic F–smectic C transitions, ▲ the smectic 2–smectic 1 transition, ◇ the smectic F–smectic A transition and + the crystal G–smectic 1 transition.

of the 10.O*n*O.10 series are several times larger than the $\Delta S_{NI}/R$ values for the 2.O*n*O.2 series. The $\Delta S_{S_AI}/R$ values of the 10.O*n*O.10 series show a large odd–even effect with the even members having the higher values and this alternation appears to be larger than that exhibited by the $\Delta S_{NI}/R$ values for the 2.O*n*O.2 series presumably reflecting an alternation in the degree of translational order present in the smectic A phases of odd and even membered dimers. It is worth noting that $\Delta S_{S_AI}/R$ for the even membered dimers is over twice that of monomeric compounds. These very large $\Delta S_{S_AI}/R$ values suggest that both the orientational and translational ordering in the smectic A phase are high for even members. This is in agreement with the X-ray diffraction data in which a second order reflection in the small angle region is often observed for the even membered dimers and implies a relatively high degree of translational order. It is impossible to interpret the relative importance of these contributions together with the conformational component to $\Delta S_{S_AI}/R$ unambiguously because all three are inter-related and so further speculation must await the results from model calculations.

3.3. *The dependence of the transitional properties on the length of the terminal chains*

Thus far the discussion has been limited to varying the spacer length *n* while holding the terminal chain length *m* constant. We shall now consider the reverse, holding *n* constant while varying *m*; the three homologous series, *m*.O4O.*m*, *m*.O5O.*m* and *m*.O12O.*m* chosen for this purpose show typical behaviour for these compounds and we should note that the behavioural trends are repeated between even to even and odd to odd series.

3.3.1. *m.O4O.m series*

Figure 16 shows the dependence of the transition temperatures on *m* for the *m*.O4O.*m* series. The nematic–isotropic transition temperature increases markedly on going from 0.O4O.0 to 1.O4O.1 although it is not apparent why the addition of a single methyl group should have such a large relative effect on T_{NI}. Subsequent increases in the length of the terminal chains cause the clearing temperatures to fall showing initially an alternation which attenuates with increasing *m*. This behaviour is typical however of a series of conventional mesogens having high clearing points [1]. As *m* increases the smectic phase stability increases as would be anticipated.

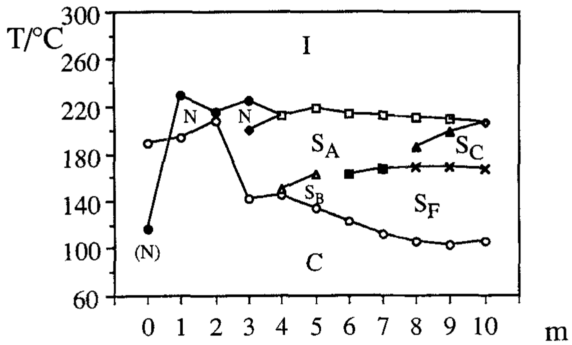

Figure 16. The dependence of the transition temperatures on the number of carbon atoms, *m*, in the terminal chains for the *m*.O4O.*m* series. Melting points are denoted by ○, ● indicate nematic–isotropic transitions, □ smectic A–isotropic transitions, ◇ the smectic C–isotropic transition, ◆ the smectic A–nematic transition, △ smectic B–smectic A transitions, ■ smectic F–smectic A transitions, × smectic F–smectic C transitions and ▲ smectic C–smectic A transitions.

It has often been observed that smectic tendencies of monomers are lost when coupled to form the dimer. If, however, we consider the monomeric analogue of 4.O4O.4 to be 2O.4 then quite the opposite is true, 2O.4 is purely nematic [18] whereas 4.O4O.4 exhibits both smectic A and B phases. Thus in this example the coupling of the monomer has resulted in enhanced smectic tendencies. It should be noted that this is not a general result for the *m*.O*n*O.*m*'s; for example, 6O.4 has a complicated phase sequence [18] whereas 4.O12O.4 is purely nematic. Using examples from other series these observations will be extended and discussed later.

3.3.2. *m.O5O.m series*

Figure 17 shows the dependence of the transition temperatures on the length of the terminal alkyl chains for the *m*.O5O.*m* series and again as *m* increases smectic phase stability increases. The clearing points alternate for small values of *m* and this attenuates on increasing *m*. The smectic A–isotropic temperatures increase on increasing *m* and this is observed in conventional mesogens possessing low transition temperatures [1].

Figure 18 shows the dependence of the entropy change associated with the clearing transitions for the *m*.O4O.*m* and *m*.O5O.*m* series. It is immediately apparent that any given member of the *m*.O4O.*m* series exhibits far higher values than the corresponding member of the *m*.O5O.*m* series. This reflects simply the large alternation in entropies we saw in varying the flexible spacer for any given length of terminal chain. The transitional entropies for the *m*.O*n*O.*m* series keeping *n* constant essentially increase with little or no alternation on varying *m* providing that similar transitions are being compared. This is in complete accord with the behaviour observed for conventional mesogens [19].

3.3.3. *m.O12O.m series*

Figure 19 shows the dependence of the transition temperatures on *m* for the *m*.O12O.*m* series; immediately apparent is the much reduced temperature range of the mesophases. This reflects the fact that the clearing point falls faster than the melting point as the spacer length is increased for a given terminal chain length. The first seven members of this series are purely nematic and the remaining purely smectic.

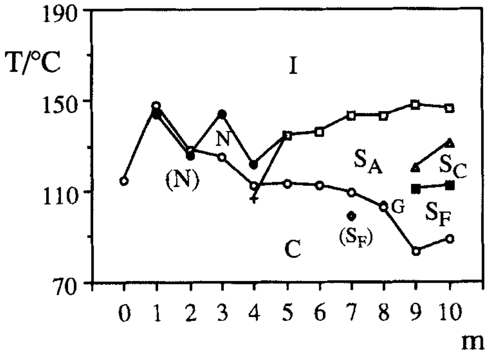

Figure 17. The dependence of the transition temperatures on the number of carbon atoms, *m*, in the terminal chains for the *m*.O5O.*m* series. Melting points are denoted by ○, ● indicate nematic–isotropic transitions, □ smectic A–isotropic transitions, + the smectic A–nematic transition, ◆ the crystal G–smectic A transition, ◇ the smectic F–smectic A transition, ■ smectic F–smectic C transitions and △ smectic C–smectic A transitions.

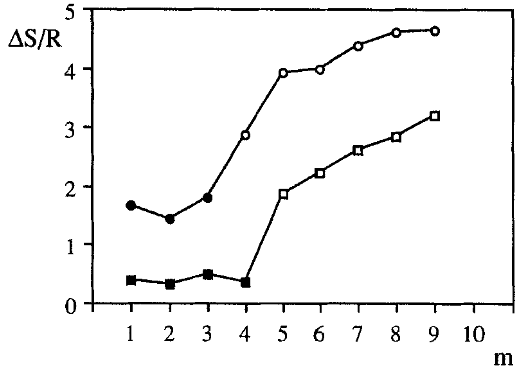

Figure 18. The dependence of the entropy change associated with the clearing point on the number of carbon atoms, *m*, in the terminal chains for the *m*.O4O.*m* (●, ○) and *m*.O5O.*m* (■, □) series. Filled symbols represent nematic–isotropic transitions and open symbols denote smectic–isotropic transitions.

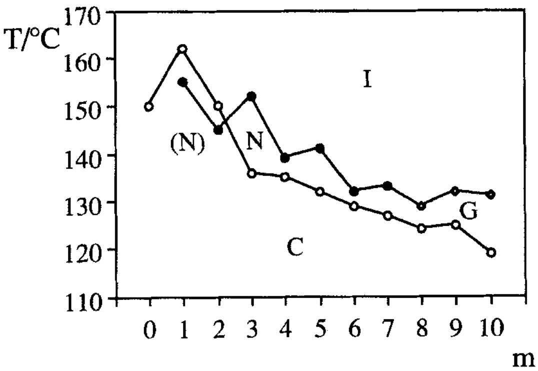

Figure 19. The dependence of the transition temperatures on the number of carbon atoms, *m*, in the terminal chains for the *m*.O12O.*m* series. ○ indicates melting points, ● nematic–isotropic transitions and ◇ crystal G–isotropic transitions.

On increasing the *m*/*n* ratio for a given series, the thermal stability of tilted smectic phases increases (see figures 16, 17 and 19). This is observed also on increasing the terminal chain lengths of monomeric materials, for example the terethalidene-bis-(4-*n*-alkylanilines) [20]. This may be the result of the terminal alkyl chains lying at an angle to the long molecular axis inducing a molecular tilt in neighbouring molecules.

3.4. *A comparison of the clearing points of the m.OnO.m series*

Figure 20 shows the dependence of the clearing temperatures on the length of the terminal alkyl chains for *m*.O*n*O.*m* series having even membered spacers. The six curves show no intersections and this reflects the trend that within a *m*.O*n*O.*m* series that the clearing points of the even members on varying the length of the spacer always lie on a decreasing curve; this can be seen in figures 10, 14 and 15. This behaviour suggests that increasing the terminal chain length serves to dilute the core–core interactions and this is expected for series having high clearing points [1]. In contrast to this behaviour figure 21 shows the dependence on *m* of the clearing points for the *m*.O*n*O.*m* series

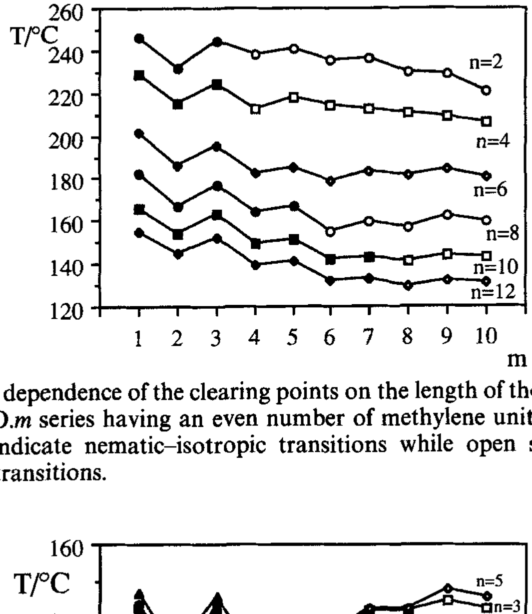

Figure 20. The dependence of the clearing points on the length of the terminal alkyl chains for the *m*.O*n*O.*m* series having an even number of methylene units in the alkyl core. Filled symbols indicate nematic–isotropic transitions while open symbols denote smectic–isotropic transitions.

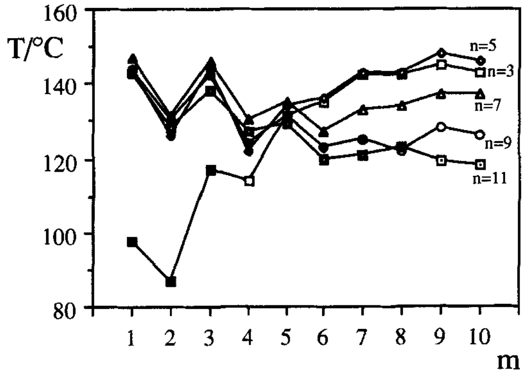

Figure 21. The dependence of the clearing points on the length of the terminal alkyl chains for the *m*.O*n*O.*m* series having an odd number of methylene units in the alkyl core. Filled symbols indicate nematic–isotropic transitions while open symbols denote smectic–isotropic transitions.

having odd membered spacers and the five curves show a far more complex behaviour involving many intersections. This reflects the fact that in a given *m*.O*n*O.*m* series on varying *n* while holding *m* constant the transition temperatures of the odd members never fall on a smooth increasing or decreasing curve but instead pass through a maximum. This is clearly seen in figures 10, 14 and 15. The *m*.O3O.*m* series behaves quite differently to the others for small values of *m* by exhibiting a steeply rising liquid crystal–isotropic transition temperature curve which levels off with increasing *m*. This is similar to the behaviour seen in conventional low molar mass liquid crystals possessing low transition temperatures [1]. The complicated behaviour seen in figure 21 presumably implies that the terminal chains are not only diluting core–core interactions but also increase the molecular anisometry. This dual role of terminal alkyl chains is well-documented in conventional low molar mass mesogens [21].

3.5. *The smectic A–nematic transition*

The smectic A–nematic transition is observed to be first order for all the dimers studied although the strength of the transition is found to vary significantly with the molecular structure (see the table). For conventional mesogens the strength of this transition as reflected by the transitional entropy, $\Delta S_{S_AN}/R$, is predicted by the McMillan theory [22] to increase as the nematic range decreases. This dependence is best revealed by a plot of $\Delta S_{S_AN}/R$ against the so-called McMillan parameter which is the ratio of the transition temperatures T_{S_AN}/T_{NI}. As this ratio increases so the transitional entropy decreases until a tricritical point is reached at which the S_A–N transition is second order. Although the McMillan theory and its variants [23] were originally developed for rigid molecules with cylindrical symmetry it is nonetheless of interest to see how our results for the mesogenic dimers compare with the theoretical predictions. We have, therefore, plotted $\Delta S_{S_AN}/R$ against T_{S_AN}/T_{NI} for dimers with both odd and even spacers with the result shown in figure 22. It is immediately apparent that as T_{S_AN}/T_{NI} decreases so the S_A–N transition weakens in much the same way as observed for conventional mesogens, for example the cholesteryl *n*-alkanoates [24] and binary mixtures of 4,4′-di-*n*-alkylazoxybenzenes [25]. Of particular interest is the observation that for this transition dimers with even and odd spacers appear to behave

The entropies associated with the smectic A–nematic transition, $\Delta S_{S_AN}/R$.

Compound	T_{S_AN}/T_{NI}	$\Delta S_{S_AN}/R$
3.O2O.3	0·992	1·08
3.O4O.3	0·950	0·12
4.O5O.4	0·962	0·20
4.O6O.4	0·965	0·18
5.O6O.5	0·996	0·49
5.O7O.5	0·961	0·15
5.O8O.5	0·952	0·10
6.O7O.6	0·999	1·06
6.O9O.6	0·967	0·12
7.O9O.7	0·990	0·44
7.O10O.7	0·993	0·34
8.O11O.8	0·990	0·42

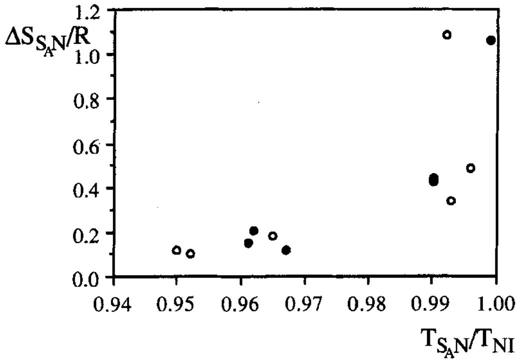

Figure 22. The dependence of $\Delta S_{S_AN}/R$ on T_{S_AN}/T_{NI} for *m*.O*n*O.*m* compounds; ○ represent dimers with an even membered spacer while ● denotes dimers having an odd membered spacer.

in essentially the same way, in marked contrast to the N–I transition. The molecular significance of this result is not immediately apparent because within this class of materials the size of the core as well as the length of the terminal chains are being varied. A proper analysis would require the development of a complete molecular field theory of the smectic A–nematic transition which allows for the flexibility of both the spacer and the terminal chains. We note that a start has been made but that the complexity of the problem has necessitated a number of major approximations [26]. By the same token we shall not attempt to interpret the relatively high tricritical temperatures implied in figure 22 for these materials.

3.6. *The smectic behaviour of dimers*

The formation of a smectic phase may be thought of as a microphase separation in which the mesogenic cores form one region while the alkyl chains constitute another. There are two major forces responsible for such a separation; energetically, the mean of the core–core and chain–chain interactions is more favourable than the mixed core–chain interaction and entropically, the interaction between a core and a chain acts to order the chain and hence is unfavourable. The very general observation for monomeric liquid crystals is that increasing the chain length in a given homologous series promotes smectic behaviour [5]. There are, however, exceptions to this rule, most notably the *trans*-4-(*trans*-4-*n*-alkylcyclohexyl)cyclohexylcarbonitriles [27]

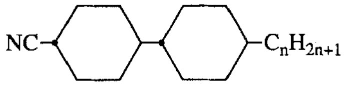

for which smectic behaviour is observed for $n=2$–5 while the heptyl homologue exhibits only a nematic phase. This suggests the presence of strong lateral interactions between the molecules which promote smectic behaviour even for short terminal chain lengths while packing considerations become increasingly important as the chain length is increased. A second exception to the general rule are the α-(4-*n*-alkylanilinebenzylidene-4′-oxy)ω-(4-cyanobiphenyl-4′-oxy)hexanes [28]

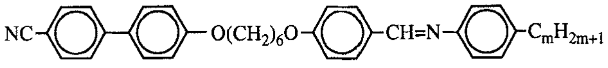

for which smectic behaviour is observed for short terminal chain lengths, $m=0$–6, and also, for $m=10$ but for $m=7$, 8 and 9 only nematic behaviour is observed. The unusual behaviour for the latter compounds was shown to be a result of the formation of differing smectic A phases. For short chain lengths the smectic A phase has an intercalated structure possibly stabilized by a specific interaction between the unlike mesogenic groups, while for $m = 10$ the smectic A phase is interdigitated, stabilized by the electrostatic interaction between the polar and polarizable cyanobiphenyl groups. In addition to these exceptions it is interesting to note that sexiphenyl [29] which possesses no terminal chains

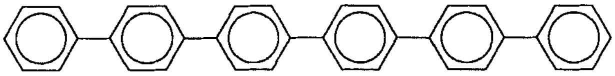

exhibits smectic behaviour suggesting that again it is the strong lateral interactions that are responsible for smectic phase formation. A computer simulation study of a system of particles interacting via the Gay–Berne potential has shown that the introduction of lateral interactions does indeed promote smectic behaviour [30]. We should also mention the filled smectic phases exhibited by mixtures for which the driving force for smectic phase formation appears to be largely a steric one in which the molecules simply pack in the most efficient manner [31]. Figure 23 shows the dependence of T_{SN} and T_{SI} on m for each m.OnO.m series. It is clear that as n is increased, the onset of smectic behaviour shifts towards larger values of m. For example, in the m.O2O.m series smectic behaviour is observed for 3.O2O.3 while for the m.O9O.m series, 6.O9O.6 is the first member to exhibit smectic behaviour. On examining the wealth of data given in the Appendix a simple empirical rule seems to emerge relating the molecular structure to the occurrence of smectic behaviour, namely, if a dimer is to exhibit smectic properties then the terminal chain length must be greater than half the spacer length; there is no exception to this rule in the m.OnO.m family. This relationship is shown in figure 24 which gives the dependence of the ratio m/n on n for the first member in each series to exhibit smectic behaviour. Also shown in figure 24 is the dependence of m/n on n for the monomeric nO.m compounds [18, 32] and it is apparent that the m/n ratio for which smectic behaviour is first observed is considerably smaller than that for the dimers. It should be noted, however, that 1O.8 and 2O.8 are both solely nematogenic and so the curve shown in figure 24 must rise very steeply as n is decreased. Also, there is some doubt as to which member of the 3O.m series is the first to exhibit smectic behaviour; Smith *et al.* [32] reported that 3O.4 exhibits a monotropic smectic phase which was not observed in the later investigation by Goodby *et al.* [18]. These differences between the dimers and monomers are difficult to interpret although it is interesting to note that

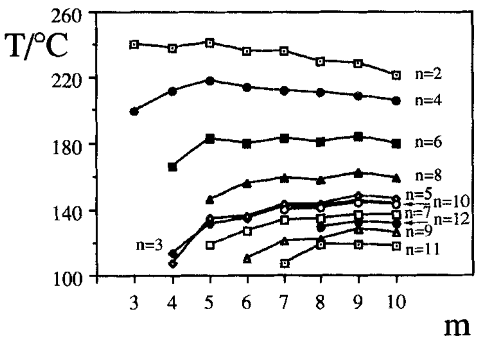

Figure 23. The dependence of the smectic–nematic or smectic–isotropic transition temperatures on the length of the terminal chains for the m.OnO.m series.

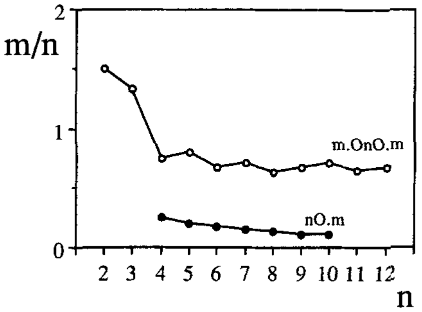

Figure 24. The dependence of the ratio of the length of the terminal chains to that of the spacer, m/n, on n for the first member in each m.OnO.m series to exhibit smectic behaviour. Also shown are the same values denoted by ● for the monomeric nO.m series.

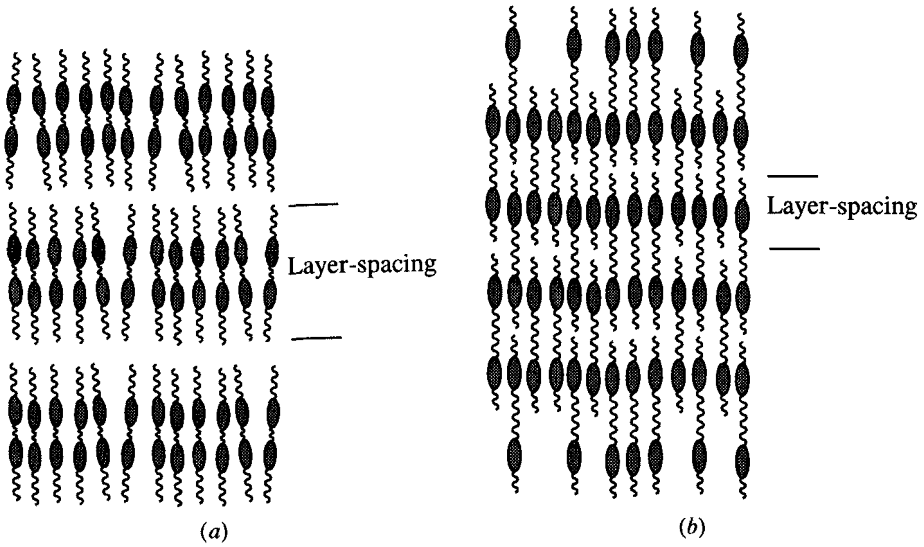

Figure 25. The structure of (*a*) the monolayer smectic A phase and (*b*) the intercalated smectic A phase.

smectic formation for these dimers involves microphase separation into three regions unlike the biphasic system described for typical monomeric compounds. The X-ray diffraction studies on these materials showed that the smectic phases have a monolayer structure (see figure 25 (*a*)) and thus the mesogenic groups, terminal chains and spacers each constitute a microphase. It is easy to imagine that for materials such as 3.O8O.3 the molecules could assemble into an intercalated structure (see figure 25 (*b*)) in which the spacers and terminal chains are mixed. However, for such a phase to form the terminal chain length would have to be half the spacer length and we have already seen that for smectic behaviour to be observed $m > n/2$. In addition if such a phase formed it could easily be distinguished from the monolayer structure in that the layer spacing would correspond to approximately half the molecular length. The mesogen–mesogen interactions are the same for both the monolayer and intercalated structures and thus, this suggests that the terminal chain-spacer interaction is an unfavourable one so destabilizing the molecular arrangement shown in figure 25 (*b*). If we consider the spacer not as a chain, therefore, but as part of the overall mesogenic unit then for a given value of *m* increasing *n* serves to increase the mesogen–mesogen interactions so diluting the influence of the smectic promoting chains. This effect of reducing molecular inhomogeneity by increasing the size of the core resulting in reduced smectic tendencies is well-documented in monomeric mesogens [5]. This interpretation suggests that the empirical rule we have noted, therefore, that $m > n/2$ for smectic phases to be observed may be accidental although as we will see it holds true for the vast majority of dimeric liquid crystals reported in the literature. This discussion has made no reference to the type of anisometric unit present in the dimer and so it would be reasonable to assume that these observations should hold true for all dimeric liquid crystals possessing terminal alkyl chains. The vast majority of this class of compounds do indeed behave in a similar fashion (see, for example [33]). The notable exceptions to this are asymmetric dimers to which we have already referred. In fact there are just three exceptions to our empirical rule relating molecular structure in symmetric dimers to smectic behaviour. The first of these are the dimeric esters described by Jin *et al.* [34]

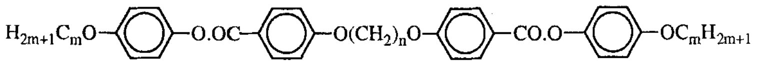

$n = 5, 6, 10$; $m = 1$–7.

The series having pentyl and hexyl spacers follow the trends revealed for the *m*.O*n*O.*m* compounds. The compounds with the hexyl spacer are nematic for small values of *m* and as *m* is increased smectic properties appear. The pentyl series is a little unusual in that all the members of the series are smectic even for short terminal chain lengths. It is the series with a decamethylene spacer, however, that disobeys the rules developed using the *m*.O*n*O.*m* series; for this series it is the short terminal chain lengths which exhibit smectic phases and as the terminal chain lengths are increased nematic properties emerge. This behaviour opposes the very general observation that smectic properties increase with increasing terminal chain length [5] and the authors offer no explanation for this unusual trend [34]. The two other exceptions both possess very long spacers [35, 36]

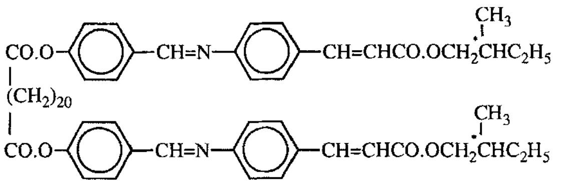

and

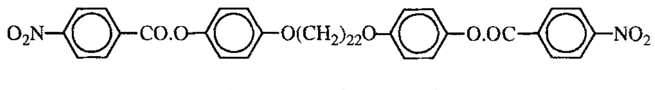

The chiral dimer [35] exhibits a ferroelectric smectic C phase as well as a smectic A phase and the smectic behaviour may be the result of the methyl branch which often promotes smectic over nematic behaviour [5]. The nitrophenylbenzoate ester [36] exhibits a highly ordered smectic phase for which the layer spacing, 29 Å, is considerably less than the estimated molecular length of 50 Å. The authors proposed a highly tilted structure which appears unrealistic in that the molecules do not interdigitate as would be expected for such polar species. A more realistic structure is presumably one with a smaller tilt angle and in which the molecules interdigitate. The driving force for smectic formation is unclear although may involve polar interactions.

Finally, we have noted that for semi-flexible main chain liquid-crystalline polymers that increasing the spacer length increases the smectic tendencies of the polymer [17] whereas the reverse is true for dimeric liquid crystals for which increasing spacer length decreases the smectic tendencies of the mesogen. This suggests that the driving force for smectic phase formation differs for the two systems and for the polymers the driving force must be an entropic one in order to disentangle the polymer chains.

4. Summary

Eleven series of the *m*.O*n*O.*m* family of compounds have been synthesized and shown to exhibit a rich smectic polymorphism. We have identified several examples of rare phase transitions, for example, the smectic F–smectic A and the crystal G–isotropic transitions as well as examples of modulated smectic phases. We believe, therefore, that these compounds are valuable for physical studies of the structures of smectic phases and also, of phase transitions. Many of the transitional properties of these dimers depend strongly on the length and parity of the spacer. In particular, the nematic–isotropic transition temperatures and entropies exhibit a marked alternation on increasing the spacer length. This alternation has been interpreted in terms of the alternation in the long range orientational order. In contrast, at the smectic A–nematic transition dimers having odd and even membered spacers behave in a similar fashion although the molecular significance of this is unclear. Finally, the dependence of the formation of smectic phases upon the length of the flexible spacer is unusual in that increasing the spacer length promotes nematic behaviour. This is unlike increasing the length of an alkyl chain in monomeric mesogens or increasing the spacer length in main chain liquid crystal polymers. An explanation of this unusual behaviour was provided by considering the formation of a smectic phase in terms of a microphasic separation into three regions but further speculation must await the results from model calculations which allow for molecular flexibility.

We are grateful to Dr A. P. J. Emerson for assistance with the molecular field theory calculations. We also wish to thank the Royal Commission for the Exhibition of 1851 for the award of a fellowship to Dr C. T. Imrie and the Science and Engineering Council for a research studentship for Dr R. W. Date as well as for a grant, GR/C/95428, towards the cost of the equipment used in this investigation.

Appendix

Table A1. The transition temperatures and entropies of transition for the 0.O*n*O.0 homologous series; ( ) denotes a monotropic transition.

n	T_{CI}/°C	T_{NI}/°C	$\Delta S_{\mathrm{CI}}/R$
1	138	—	11·1
2	189	—	15·3
3	133	—	20·8
4	189	(116)	12·4
5	115	—	13·5
6	166	—	18·1
7	107	—	14·7
8	160	—	22·1
9	102	—	15·6
10†	154	—	22·8
11	117	—	19·2
12	150	—	26·1

† Literature value; T_{CI} 153°C [6].

Table A2. The transition temperatures and entropies of transition for the 1.O*n*O.1 homologous series; ( ) denotes a monotropic transition.

n	$T_{\mathrm{C-}}$/°C	T_{NI}/°C	$\Delta S_{\mathrm{C-}}/R$	$\Delta S_{\mathrm{NI}}/R$
1	136	—	11·5	—
2	237	246	13·1	1·27
3	163	(98)	12·1	—
4	193	229	11·1	1·66
5	148	(144)	15·4	0·38
6	177	201	14·6	1·84
7	136	147	16·0	0·65
8	171	182	18·5	2·06
9	137	144	16·6	0·81
10†	167	(166)	21·8	2·18
11	130	143	17·6	1·12
12	162	(155)	25·5	2·37

† Literature values; T_{CI} 164°C, T_{NI} 161°C [6].

Table A3. The transition temperatures and entropies of transition for the 2.O*n*O.2 homologous series; ( ) denotes a monotropic transition.

n	T_{C-}/°C	T_{NI}/°C	$\Delta S_{C-}/R$	$\Delta S_{NI}/R$
1	136	—	9·00	—
2	230	232	12·5	0·97
3	153	(87)	12·4	—
4	208	215	10·3	1·45
5	128	(126)	13·3	0·32
6	160	186	12·6	1·52
7	116	131	14·1	0·46
8	154	167	16·1	1·81
9	112	130	16·4	0·64
10	151	154	19·2	1·89
11	112	128	17·8	0·86
12	150	(145)	23·4	2·00

Table A4. The transition temperatures and entropies of transition for the 3.O*n*O.3 homologous series; ( ) denotes a monotropic transition.

n	T_{C-}/°C	T_{S_AN}/°C	T_{NI}/°C	$\Delta S_{C-}/R$	$\Delta S_{S_AN}/R$	$\Delta S_{NI}/R$
1	133	—	—	8·43	—	—
2	220	240	244	11·6	1·08	1·92
3	148	—	(117)	11·5	—	—
4	141	199	224	11·2	0·12	1·80
5	125	—	144	10·9	—	0·50
6	145	—	195	13·3	—	1·82
7	114	—	146	13·3	—	0·72
8	145	—	177	15·5	—	2·10
9	118	—	142	16·4	—	0·82
10	137	—	163	17·1	—	2·18
11	109	—	138	12·1	—	0·95
12	136	—	152	17·0	—	2·25

Table A5. The transition temperatures and entropies of transition for the 4.O*n*O.4 homologous series; ( ) denotes a monotropic transition.

		$T_{S_BS_A}$/°C†	T_{S_AI}/°C†		$\Delta S_{S_BS_A}/R$†	$\Delta S_{S_AI}/R$†
n	T_{C-}/°C	T_{S_AN}/°C	T_{NI}/°C	$\Delta S_{C-}/R$	$\Delta S_{S_AN}/R$	$\Delta S_{NI}/R$
1	131	—	—	8·20	—	—
2	204	—	238†	11·9	—	2·89†
3	141	—	(114)†	11·3	—	—
4	145	150†	212†	9·22	1·48†	2·88†
5	112	(107)	122	8·14	0·20	0·37
6	140	166	182	12·7	0·18	1·78
7	110	—	130	14·1	—	0·62
8	137	—	164	16·0	—	2·00
9	108	—	124	14·2	—	0·66
10	135	—	149	17·9	—	2·04
11	104	—	127	15·2	—	0·78
12	135	—	139	17·5	—	2·11

Table A6. The transition temperatures and entropies of transition for the 5.O*n*O.5 homologous series; ( ) denotes a monotropic transition.

				T_{S_AI}/°C†				$\Delta S_{S_AI}/R$†
n	T_{C-}/°C	$T_{S_BS_A}$/°C	T_{S_AN}/°C	T_{NI}/°C	$\Delta S_{C-}/R$	$\Delta S_{S_BS_A}/R$	$\Delta S_{S_AN}/R$	$\Delta S_{NI}/R$
1	128	—	—	—	7·80	—	—	—
2	197	—	—	241†	11·9	—	—	3·68†
3	138	—	—	(131)†	10·9	—	—	1·73†
4	133	162	—	218†	9·22	1·72	—	3·92†
5	113	—	—	134†	9·09	—	—	1·85†
6	134	(129)	183	185	13·1	0·65	0·49	2·42
7	115	—	119	135	14·2	—	0·15	0·79
8	131	—	146	167	15·9	—	0·10	2·57
9	103	—	—	131	16·5	—	—	1·09
10	131	—	—	151	19·6	—	—	2·72
11	106	—	—	129	18·9	—	—	1·11
12	132	—	—	141	18·9	—	—	2·77

Table A7. The transition temperatures and entropies of transition for the 6.O*n*O.6 homologous series; ( ) denotes a monotropic transition.

n	$T_{C-}/°C$	$T_{S_FS_A}/°C$	$T_{S_AN}/°C$	$T_{S_AI}/°C$ $T_{NI}/°C†$	$\Delta S_{C-}/R$	$\Delta S_{S_FS_A}/R$	$\Delta S_{S_AN}/R$	$\Delta S_{S_AI}/R$ $\Delta S_{NI}/R†$
1	125	—	—	—	9·24	—	—	—
2	194	—	—	236	11·8	—	—	3·81
3	135	—	—	(135)	11·4	—	—	2·12
4	123	162	—	214	8·20	1·68	—	4·00
5	112	—	—	136	9·65	—	—	2·21
6	124	137	—	179	9·80	1·85	—	3·81
7	114	—	127	127†	14·5	—	1·06	0·97†
8	128	—	—	155	15·2	—	—	3·68
9	105	—	110	123†	15·7	—	0·12	0·74†
10	130	—	—	142†	18·8	—	—	2·28†
11	105	—	—	120†	18·3	—	—	0·77†
12	129	—	—	132†	16·7	—	—	1·94†

Table A8. The transition temperatures and entropies of transition for the 7.O*n*O.7 homologous series; ( ) denotes a monotropic transition.

n	$T_{C-}/°C$	$T_{S_CS_A}/°C†$ $T_{S_FS_A}/°C$ $T_{GS_A}/°C‡$ $T_{GN}/°C§$	$T_{S_AN}/°C$	$T_{S_AI}/°C$ $T_{NI}/°C†$	$\Delta S_{C-}/R$	$\Delta S_{S_FS_A}/R$ $\Delta S_{GS_A}/R†$ $\Delta S_{GN}/R‡$	$\Delta S_{S_AN}/R$	$\Delta S_{S_AI}/R$ $\Delta S_{NI}/R†$
1	125	—	—	—	11·6	—	—	—
2	190	211†	—	236	11·1	—	—	4·00
3	132	—	—	142	9·26	—	—	2·50
4	112	166	—	212	7·79	1·15	—	4·38
5	109	(99)	—	143	9·72	2·99	—	2·62
6	115	144	—	183	10·8	1·97	—	4·63
7	115	—	—	133	15·0	—	—	2·52
8	133	133	—	159	16·1	4·51	—	4·50
9	107	(101)‡	121	125†	15·3	11·9†	0·44	0·96†
10	125	130‡	140	143†	13·1	5·20†	0·34	2·50†
11	103	107§	—	121†	12·7	8·71‡	—	1·54†
12	127	—	—	133†	18·6	—	—	2·86†

Table A9. The transition temperatures and entropies of transition for the 8.O*n*O.8 homologous series; ( ) denotes a monotropic transition.

n	T_{C-}/°C	$T_{S_FS_C}$/°C† T_{GS_A}/°C $T_{S_FS_A}$/°C§	$T_{S_CS_A}$/°C T_{S_AN}/°C‡	T_{S_AI}/°C T_{NI}/°C‡ T_{GI}/°C§	$\Delta S_{C-}/R$	$\Delta S_{S_FS_C}/R$‡ $\Delta S_{GS_A}/R$ $\Delta S_{S_FS_A}/R$§	$\Delta S_{S_AI}/R$ $\Delta S_{NI}/R$‡ $\Delta S_{GI}/R$§
1	121	—	—	—	10·5	—	—
2	183	—	225	230	10·6	—	4·33
3	127	—	—	142	9·09	—	2·61
4	106	169†	186	211	16·3	2·00‡	4·61
5	103	104	—	143	9·42	2·93	2·85
6	112	145†	146	181	10·9	2·59‡	4·77
7	116	(102)	—	134	15·4	3·42	2·88
8	128	136§	—	157	13·4	2·74§	5·04
9	110	(106)	—	122	16·7	4·48	2·99
10	123	133	—	141	13·1	4·83	5·25
11†	99	117	119‡	123‡	11·3	7·48	1·04‡
12	124	—	—	129§	14·3	—	9·78§

† $\Delta S_{S_AN}/R = 0{\cdot}42$.

Table A10. The transition temperatures and entropies of transition for the 9.O*n*O.9 homologous series; ( ) denotes a monotropic transition.

n	T_{C-}/°C	$T_{S_FS_C}$/°C	$T_{S_CS_A}$/°C $T_{S_FS_A}$/°C† T_{GS_A}/°C‡	T_{S_CI}/°C† T_{S_AI}/°C T_{GI}/°C‡	$\Delta S_{C-}/R$	$\Delta S_{S_FS_C}/R$	$\Delta S_{S_FS_A}/R$ $\Delta S_{GS_A}/R$†	$\Delta S_{S_CI}/R$† $\Delta S_{S_AI}/R$ $\Delta S_{GI}/R$‡
1	120	—	—	—	11·6	—	—	—
2	182	—	—	229†	10·3	—	—	4·41†
3	125	—	132	145	9·02	—	—	2·99
4	103	169	198	209	8·55	1·81	—	4·65
5	83	111	120	148	8·30	3·08	—	3·20
6	106	151	161	184	11·8	4·69	—	5·25
7	105	—	113†	137	11·8	—	3·66	3·52
8	123	—	142†	162	13·9	—	2·79	5·59
9	108	—	113†	128	12·0	—	4·32	3·56
10	128	—	136†	144	15·5	—	3·69	5·58
11	115	—	117‡	119	10·8	—	6·40†	2·85
12	125	—	—	132‡	13·2	—	—	7·95‡

Table A11. The transition temperatures and entropies of transition for the 10.O*n*O.10 homologous series; ( ) denotes a monotropic transition.

n	$T_{C-I}/°C$	$T_{S_FS_C}/°C$ $T_{S_2S_1}/°C†$ $T_{S_FS_A}/°C‡$ $T_{GS_1}/°C§$	$T_{S_CS_A}/°C$ $T_{S_1S_A}/°C†$	$T_{S_CI}/°C†$ $T_{S_AI}/°C$ $T_{GI}/°C‡$	$\Delta S_{C-I}/R$	$\Delta S_{S_FS_C}/R$ $\Delta S_{S_FS_A}/R†$ $\Delta S_{GS_1}/R‡$	$\Delta S_{S_1S_A}/R$	$\Delta S_{S_CI}/R†$ $\Delta S_{S_AI}/R$ $\Delta S_{GI}/R‡$
1	119	—	—	—	14·4	—	—	—
2	175	—	—	221†	11·7	—	—	5·03†
3	120	(112)	135	143	8·90	—	—	3·10
4	105	167	—	206†	17·6	4·10	—	5·29†
5	89	112	131	146	10·9	3·62	—	3·53
6	103	149	171	180	14·1	4·20	—	4·99
7	106	114	118	137	17·9	3·03	—	3·10
8	116	140	142	159	13·5	2·79	—	5·48
9	105	(105)†	114†	126	12·5	—	4·60	3·91
10	124	136‡	—	143	16·0	4·00†	—	5·93
11	99	104§	116†	118	11·8	0·18‡	5·57	3·68
12	119	—	—	131‡	15·4	—	—	9·60‡

References

[1] Gray, G. W., 1979, *The Molecular Physics of Liquid Crystals*, edited by G. R. Luckhurst and G. W. Gray (Academic Press), chap. 1.

[2] Demus, D., 1990, *Liq. Crystals*, **5,** 75.

[3] Emsley, J. W., Luckhurst, G. R., Shilstone, G. N., and Sage, I., 1984, *Molec. Crystals liq. Crystals Lett.*, **102,** 223.

[4] Griffin, A. C., and Britt, T. R., 1981, *J. Am. chem. Soc.*, **103,** 4957.

[5] Gray, G. W., 1979, *The Molecular Physics of Liquid Crystals*, edited by G. R. Luckhurst and G. W. Gray (Academic Press), chap. 12.

[6] Jin, J.-I., and Park, J.-H., 1984, *Molec. Crystals liq. Crystals*, **110,** 293.

[7] Donahue, H. B., Benjamin, L. E., Fennoy, L. V., and Greiff, D., 1960, *J. org. Chem.*, **26,** 474.

[8] Keller, P., and Liebert, L., 1978, *Solid State Phys.*, Suppl., **14,** 19.

[9] Gray, G. W., and Goodby, J. W., 1984, *Smectic Liquid Crystals—Textures and Structures* (Leonard-Hill).

[10] Levelut, A. M., and Tinh, N. H., 1987, *J. Phys., Paris*, **48,** 847.

[11] Imrie, C. T., 1989, *Liq. Crystals*, **6,** 391.

[12] Attard, G. S., Garnett, S., Hickman, C. G., Imrie, C. T., and Taylor, L., 1990, *Liq. Crystals*, **7,** 495.

[13] Wiegeleben, A., Richter, L., Deresch, J., and Demus, D., 1980, *Molec. Crystals liq. Crystals*, **59,** 329.

[14] Luckhurst, G. R., Zannoni, C., Nordio, P. L., and Segre, U., 1975, *Molec. Phys.*, **30,** 1345.

[15] Luckhurst, G. R., 1985, *Recent Advances in Liquid Crystalline Polymers*, edited by L. L. Chapoy (Elsevier Applied Science Publishers), chap. 7.

[16] Emsley, J. W., Luckhurst, G. R., and Shilstone, G. N., 1984, *Molec. Phys.*, **53,** 1023.

[17] Finkelmann, H., 1987, *Thermotropic Liquid Crystals* (Critical Reports on Applied Chemistry, Vol. 22), edited by G. W. Gray (John Wiley and Sons), chap. 6.

[18] Goodby, J. W., Gray, G. W., Leadbetter, A. J., and Mazid, M. A., 1980, *Liquid Crystals of One- and Two-Dimensional Order* (Springer Series in Chem. Phys. 11), edited by W. Helfrich and G. Heppke (Springer-Verlag), p. 3.

[19] Marzotko, D., and Demus, D., 1975, *Pramana*, Suppl., **1,** 189.

[20] Kumar, S., 1981, *Phys. Rev.* A, **23,** 3207.

[21] Imrie, C. T., and Taylor, L., 1989, *Liq. Crystals*, **6,** 1.

[22] McMillan, W. L., 1971, *Phys. Rev.* A, **4,** 1238; 1972, *Ibid.*, **6,** 936.

[23] Kventsel, G. F., Luckhurst, G. R., and Zewdie, H. B., 1985, *Molec. Phys.*, **56**, 589.
[24] Barall II, E. M., and Johnson, J. F., 1974, *Liquid Crystals and Plastic Crystals*, edited by G. W. Gray and P. A. Winsor (Ellis Horwood Ltd.), p. 254.
[25] Achard, M. F., Hardouin, F., Sigaud, G., and Gasparoux, H., 1976, *J. chem. Phys.*, **65**, 1387.
[26] Mukherjee, C. D., Bose, T. R., Ghosh, D., Roy, M. K., and Saha, M., 1985, *Molec. Crystals. liq. Crystals*, **124**, 139.
[27] Brownsey, G. J., and Leadbetter, A. J., 1981, *J. Phys. Lett., Paris*, **42**, 135.
[28] Hogan, J. L., Imrie, C. T., and Luckhurst, G. R., 1988, *Liq. Crystals*, **3**, 645.
[29] Irvine, P. A., Wu, D. C., and Flory, P. J., 1984, *J. chem. Soc. Faraday Trans. 1*, **80**, 1795.
[30] Luckhurst, G. R., Stephens, R. A., and Phippen, R. W., 1990, *Liq. Crystals*, **8**, 451.
[31] Pelzl, G., Humke, A., Diele, S., Demus, D., and Weissflog, W., 1990, *Liq. Crystals*, **7**, 115.
[32] Smith, G. W., Gardlund, Z. G., and Curtis, R. J., 1973, *Molec. Crystals liq. Crystals*, **19**, 327.
[33] Centore, R., Roviello, A., and Sirigu, A., 1988, *Liq. Crystals*, **3**, 1525.
[34] Jin, J.-I., Oh, H.-T., and Park, J.-H., 1986, *J. chem. Soc. Perkin Trans, 2*, 343.
[35] Shiraishi, K., Kato, K., and Sugiyama, K., 1990, *Chem. Lett.*, 971.
[36] Poeti, G., Fanelli, E., and Guillon, D., 1990, *Thermochim. Acta*, **164**, 251.